THE RADIOACTIVE DECAY OF IRIDIUM-186

DISSERTATION

Presented in Partial Fulfillment of the Requirements for the Degree of Doctor of Philosophy in the Graduate School of The Ohio State University

By

Binayak Ghosh, B.Sc., M.Sc.

The Ohio State University
1962

Approved by

M. L. Pool

Adviser
Department of Physics
and Astronomy

ACKNOWLEDGMENTS

I take this opportunity to express my sincere gratitude to my adviser Professor M. L. Pool for his constant guidance throughout the length of this work.

I also thank Mr. R. W. Bailey, Mr. U. W. Ludwig, Mr. R. H. Kelley,and Mr. R. P. Sullivan of this laboratory for their kind co-operation during experimentation and otherwise. I am particularly grateful to Mr. Paul Measel for the instrumentation of the coincidence measurements.

TABLE OF CONTENTS

LIST OF TABLES

LIST OF FIGURES

1. INTRODUCTION

The energy of a rotational state of spin I in an even mass nucleus is given by[1],

$$E_I = E_0 + \frac{\hbar^2}{2J} I(I+1)$$

where E_0 is the zero point energy.

The level sequence for levels with $K \neq 0$ is I, I+1, I+2, etc. For $K=0^+$, levels with paired particle configurations have level sequence 0^+, 2^+, 4^+, etc. For $K=0^+$, it is a characteristic of the rotational spectrum that the excitation of a high member is followed by a cascade of E2 gamma transitions with energy values in the ratio ····· 15:11:7:3 and with no cross overs.[2]

Nuclei in the region $64 < Z < 74$ show a characteristic rotational structure. Also, for $155 < A < 185$ and $A > 225$ the small excitation energies suggest a strong coupling. Tungsten with Z=74 demonstrates well-defined rotational bands. Nuclei with $Z \geqslant 78$ lying near to the closed shell structure can be well described by single particle model. Thus, nuclei with $74 \leqslant Z \leqslant 78$ lie in the transitional region and a study of them may throw much light on the theories of single particle and collective models of nuclei.

The objective of this work is to find the mode of decay of ${}_{77}Ir^{186}_{109}$ nucleus obtained by proton bombardment of ${}_{76}Os^{186}_{110}$ and to find the excited levels of Os^{186} nucleus, observed in course of decay of Ir^{186} by electron capture and positron emission.

A 14-hour iridium activity was obtained by Smith and Hollander[3] from a decay of 2.5-hour platinum activity. Principal gamma rays were reported to be 135, 300, and 435 kev. On the basis of the systematics of levels of even-mass osmium isotopes Scharff-Goldhaber et al. ascribed the activity definitely to mass 186 and observed transitions at 137, 297, 434, 625, and 773 kev. Diamond and Hollander[4] measured K to L conversion ratios of the three lowest energy transitions— 137, 297, and 434 kev, all of which were found to be E2 transitions. Meanwhile, Metzger and Hill[5], Steffen[6], and Johns et al.[7] measured the β^--transitions of Re^{186} to Os^{186} and fitted the observed radiations 631 and 768 kev in a level scheme of Os^{186}. On the basis of this information Diamond and Hollander[4] suggested a level scheme interpreting in terms of collective excitation for even nuclei as suggested in Bohr and Mottelson.[2]

In this present work detailed study of the gamma rays in $Ir^{186} \xrightarrow[\beta^+]{\epsilon} Os^{186}$ decay was made along with gamma intensity measurement and gamma-gamma coincidence work. On the basis of these measurements a decay scheme has been suggested and an attempt has been made to interpret it in terms of collective excitation of deformed nuclei.

2. INSTRUMENTATION

Equipments used in this investigation can be broadly classified under three groups:

(a) Scintillators used as detector heads.

(b) Multichannel pulse height analyser.

(c) Coincidence arrangements.

(a) Detector heads

(1) A 3-inch diameter x 3-inch high NaI(Tl) crystal mounted on a Dumont 6363 photomultiplier tube was used for calibration of gamma energy, measurement of decay rate, and unscrambling of gamma ray spectrum. The crystal-mounting technique was followed as described by P. R. Bell et al.[14] at Oak Ridge National Laboratory and a schematic diagram of this is given in figure 1. Aluminium crystal housing of this detector absorbed all L x-rays and, thus, for L x-ray detection a separate x-ray detector had to be used. To reduce background the 3-inch x 3-inch crystal was shielded in a 4-inch thick lead cave with inner dimensions of 32 x 32 x 30 inches. The inner surface of the lead cave had a graded shield of 30 mils of tin and 10 mils of copper. A schematic diagram of the cave is shown in figure 2. Grading was necessary to reduce the effect of x-rays produced in the lead walls of the cave.[8]

(2) A 3-inch diameter x 3-inch high NaI(Tl) crystal with 3/8-inch diameter well drilled along the axis from one end up to the crystal center was also used for spectral study. The crystal was mounted on a Dumont 6364 photomultiplier tube. When a radioactive source was

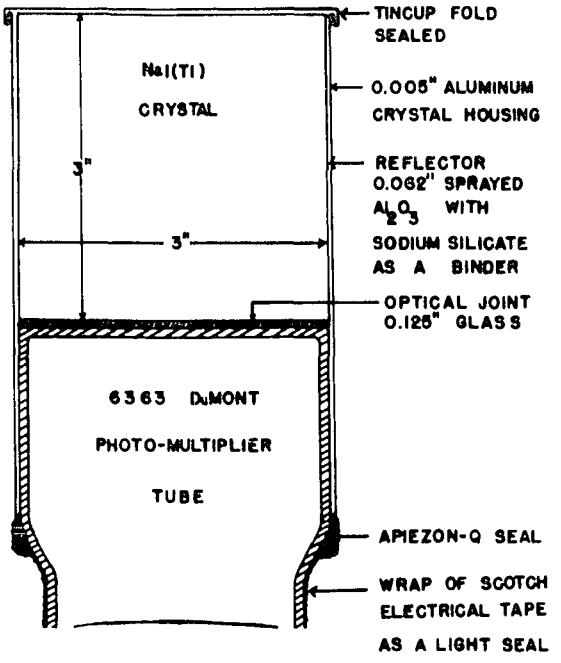

FIG. 1 3x3-inch FLAT NaI(Tl) CRYSTAL DETECTOR

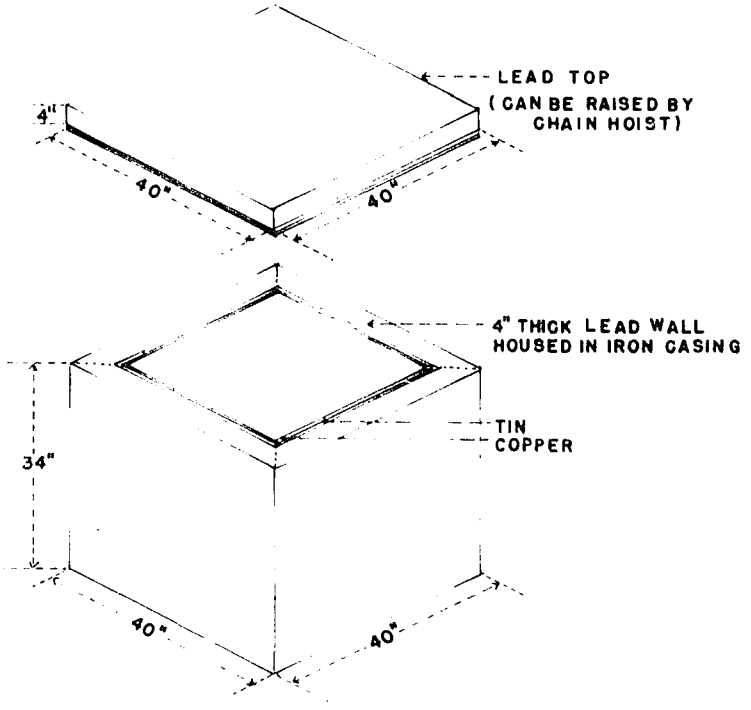

FIG. 2. LEAD CAVE

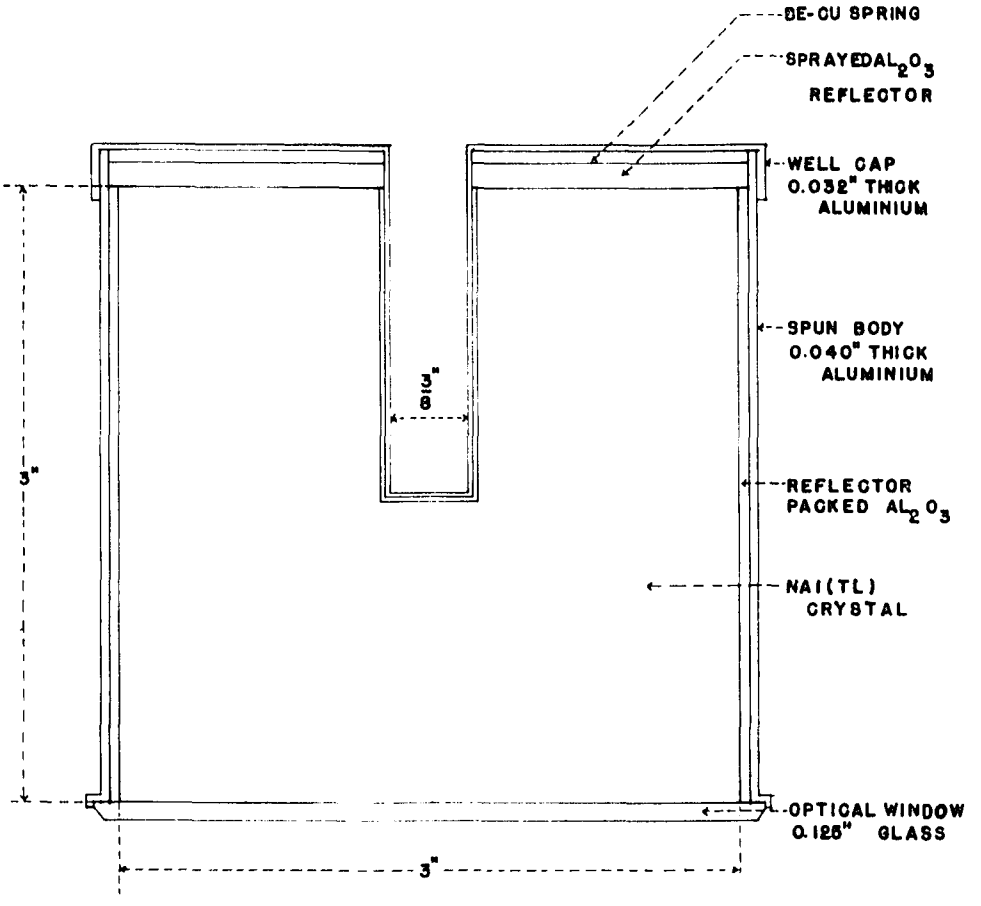

FIG.3. WELL CRYSTAL

placed inside the well, a nearly 4π geometry was obtained. The source could also be placed on the side of the crystal giving nearly a 2π geometry. The former position was called "In Well" and latter "Out Well." Comparing "In" and "Out Well" spectra the coincidence summing effect could be studied qualitatively. To reduce background the crystal assembly was placed inside a lead shield lined with a graded shield of tin and copper to eliminate the effect of x-rays produced from the lead shield itself. A scheme of the crystal assembly is shown in figure 3.

(3) Two other NaI (Tl) crystals, each 1 3/4-inch diameter x 2-inch long, were used for coincidence measurements. The crystals were mounted on two EMI 6097B photomultiplier tubes and each crystal assembly with preamplifier circuit was enclosed in a steel housing.

(4) The x-ray crystal was a 1-inch diameter x 1/4-inch thick right cylinder of NaI (Tl) and the face of acceptance was covered with 5 mils of beryllium backed by a one-micron thick aluminium reflector. This arrangement was very suitable for radiations with energies from 5 kev to about 100 kev. The crystal was mounted on a EMI 6097B photomultiplier tube.

(b) Multichannel Pulse Height Analysers

(1) The output from the 3-inch x 3-inch cave crystal, or 3-inch x 3-inch well crystal, or 1-inch x 1/4-inch x-ray crystal was analysed by a Radiation Instrument Development Laboratory Model 34-8, 200-channel pulse-height analyser. This analyser could discriminate the pulse heights, store in a magnetic memory, and print or punch out

the number of counts with their corresponding addresses. This analyser could store up to a maximum of 999,999 counts per channel and when turned in subtract mode could subtract background from the gross counts.

(2) A 400-channel R.I.D.L. Model 34-12 pulse-height analyser was used in conjunction with the 1 3/4-inch x 2-inch crystals and other coincidence circuit arrangements for coincidence experiments. Each 100 channels of the analyser constituted a subgroup and responded to a single coincidence gate. The memory of Model 34-12 had a maximum capacity of 99,999 counts per channel and in a subtract mode could subtract background or chance coincidence counts.

(c) Coincidence Arrangements

Two detectors with 1 3/4-inch x 2-inch crystals were placed face to face at 180° for coincidence work. The source was placed inside a compton shield consisting of a 5/8-inch thick lead plate with a grove inside and covered with 0.033-inch thick tin and 0.022-inch thick copper plates on both sides of lead (figure 4). This Compton shield with the source at the center was sandwiched between the detector heads.

The detector heads fed into a slow-fast coincidence circuit shown in figure 5. The resolving time of the fast coincidence circuit was analysed with a variable delay line, and a graph showing counts-delay is given in figure 6. The resolving time τ of the circuit was approximately 30×10^{-9} sec. Rate of chance coincidence, R, is,

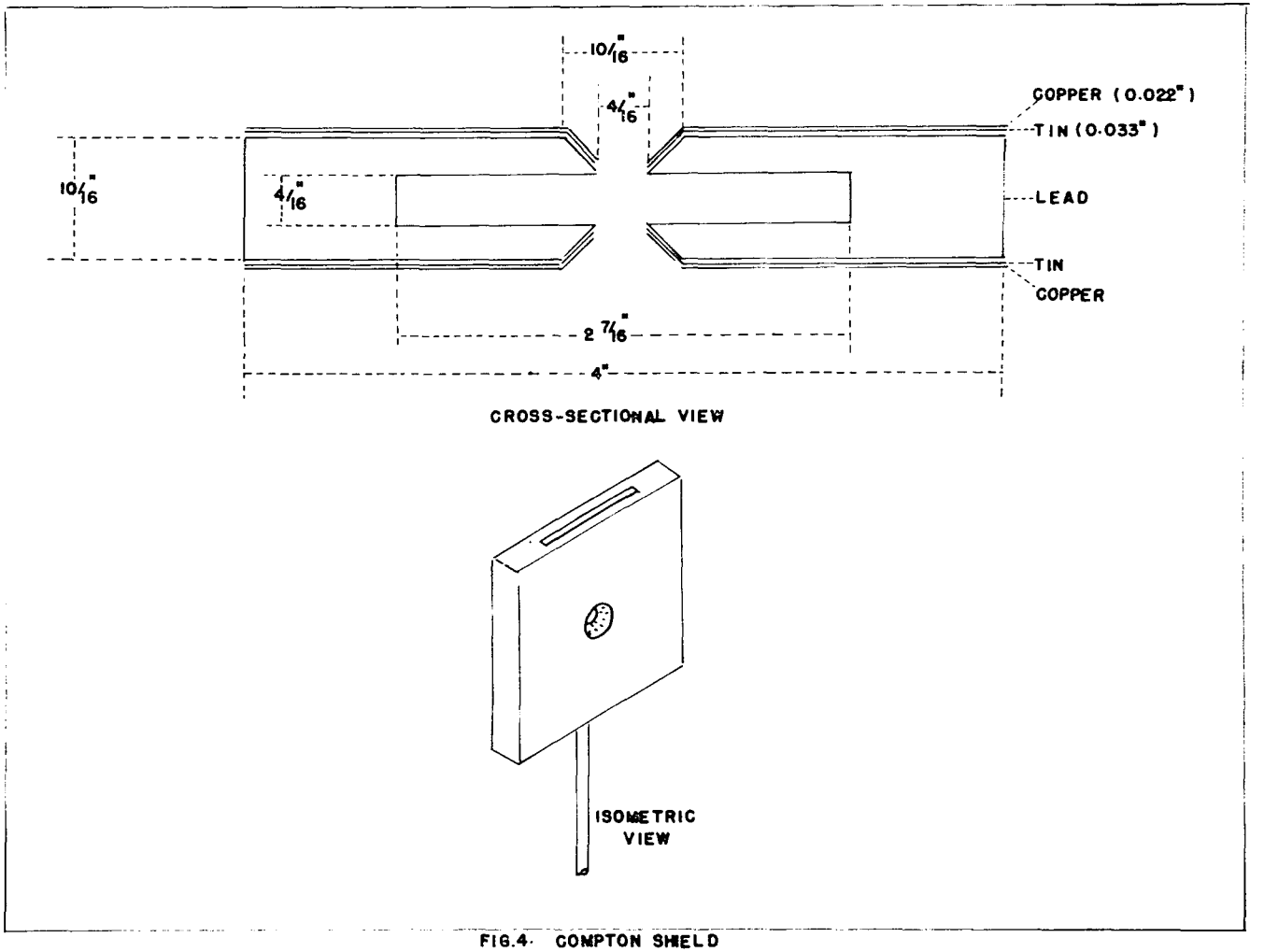

FIG.4· COMPTON SHIELD

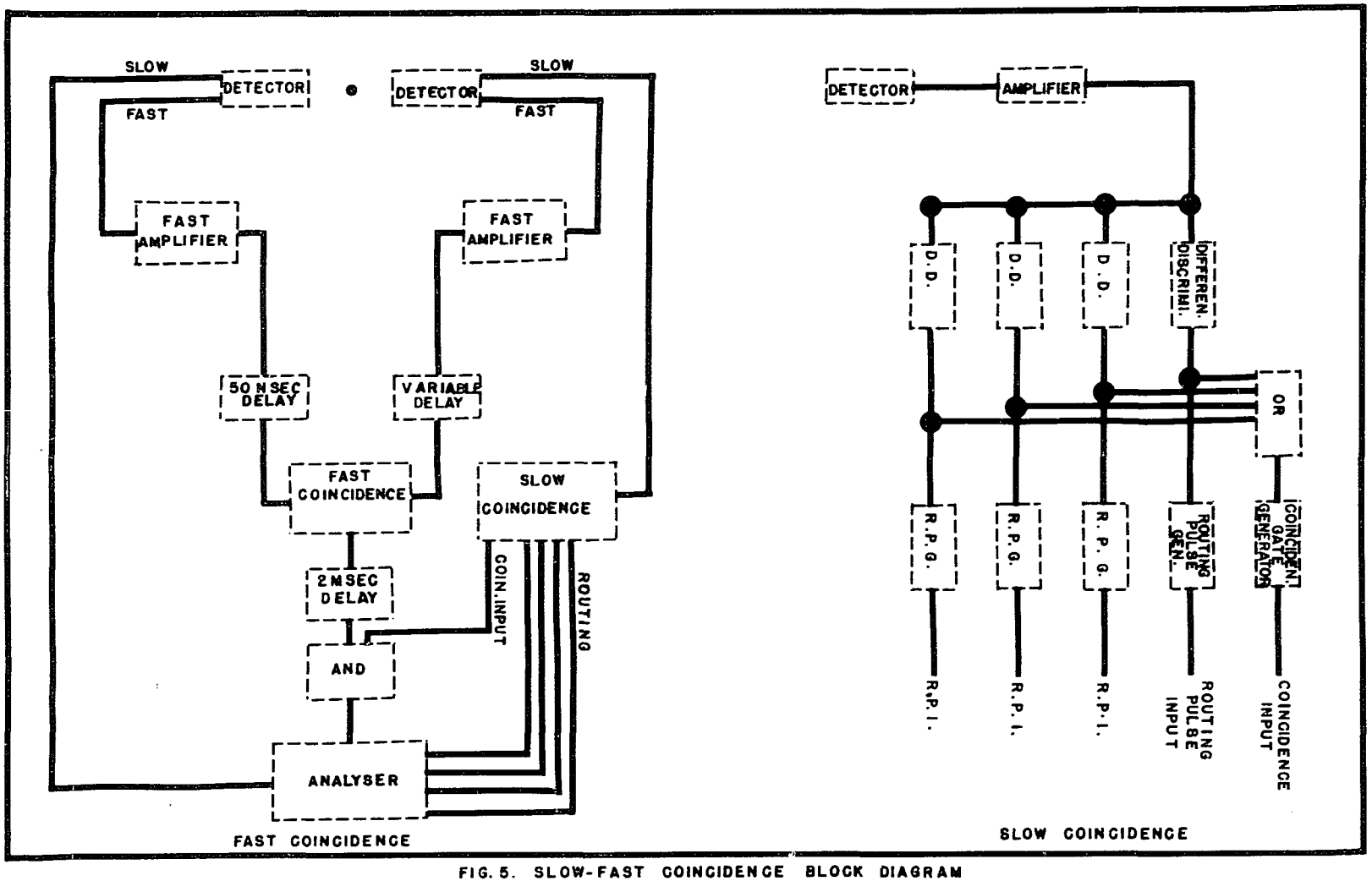

FIG. 5. SLOW-FAST COINCIDENCE BLOCK DIAGRAM

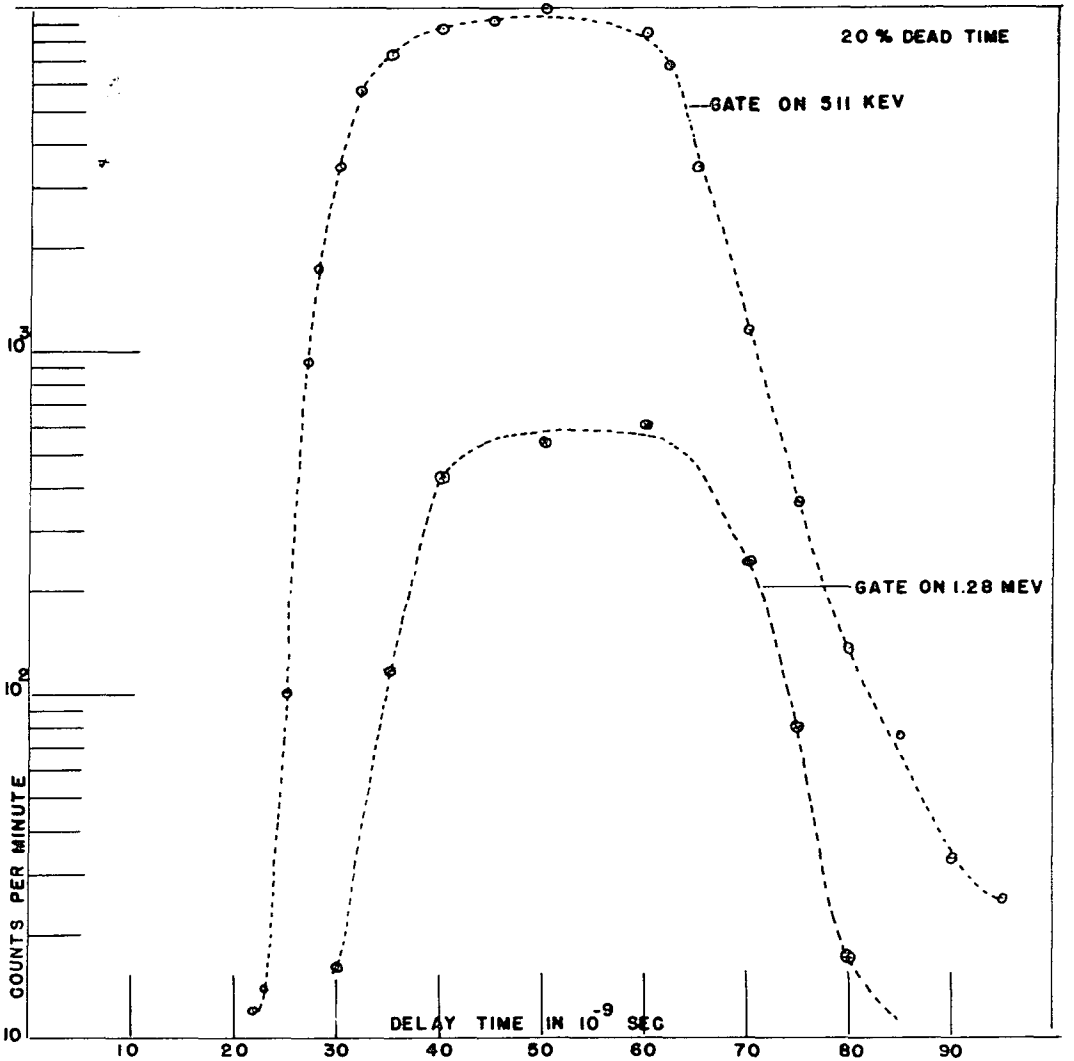

FIG. 6. RESPONSE-DELAY CURVES OF FAST COINCIDENCE CIRCUIT

$$R = 2\tau n_1 n_2$$

where, τ = resolving time,

n_1 = rate of count in coincidence gate, and

n_2 = rate of count in non-coincidence normal spectrum.

On calculation, R was found to be negligibly small and thus all the results given in this investigation are those of gross coincidence.

The coincidence circuit itself was made up of four differential discriminators, thus it was possible to set four different coincidence gates simultaneously, which in turn fed to four different sub-groups (each of 100 channels) of the 400-channel analyser. This made possible an economy of time and simultaneous comparison of different coincidence curves.

3. DECAY OF IR^{186}

(a) Qualitative Study Of Spectra

Osmium enriched in mass number 186 (Table I), obtained from O.R.N.L., was bombarded by 6 mev proton in The Ohio State University cyclotron on three different occasions and for three different lengths of bombarding time (Table III) and the resultant activities were studied independently. These three different studies produced remarkably identical decay and nature of spectra observed chronologically. It was found that (p,n) type was the only noticeable kind of reaction. On this assumption the following radioactive decays were found possible from the above isotope enriched in mass 186.

$$0.1\%\ Os^{184}(p,n)\ Ir^{184} \xrightarrow[(3\ h)]{\epsilon,\ \beta^+} Os^{184}\ (\text{stable})$$

$$61.27\%\ Os^{186}(p,n)\ Ir^{186} \xrightarrow[(15\ h)]{\epsilon,\ \beta^+} Os^{186}\ (\text{stable})$$

$$3.31\%\ Os^{187}(p,n)\ Ir^{187} \xrightarrow[(12\ h)]{\epsilon} Os^{187}\ (\text{stable})$$

$$9.54\%\ Os^{188}(p,n)\ Ir^{188} \xrightarrow[(41\ h)]{\epsilon,\ \beta^+} Os^{188}\ (\text{stable})$$

$$7.31\%\ Os^{189}(p,n)\ Ir^{189} \xrightarrow[(11\ d)]{\epsilon} Os^{189}\ (\text{stable})$$

$$8.77\%\ Os^{190}(p,n)\ Ir^{190} \begin{cases} \xrightarrow[(3.2\ h)]{\epsilon,\ \beta^+} Os^{190}\ (\text{stable}) \\ \xrightarrow[(11\ d)]{\epsilon} Os^{190}\ (\text{stable}) \end{cases}$$

$$9.8\%\ Os^{192}(p,n)\ Ir^{192} \begin{cases} \xrightarrow{\epsilon,\ \beta^+} Os^{192}\ (\text{stable}) \\ \xrightarrow[(75\ d)]{\beta^-} Pt^{192}\ (10^{15}\ y) \end{cases}$$

Proton capture reaction, if it occurred at all, could produce a few more stable iridium isotopes Ir^{191}(stable) and Ir^{193}(stable) along with a negligibly small 15 h Ir^{185} activity from Os^{184}(0.1%) and thus could be expected to produce no visible result.

Table I. Composition Of Osmium Isotopes

Enriched In Mass Number 186

Isotopic Analysis			Spectrographic Analysis	
Isotope	Atomic %	Precision	Element	%
184	0.1	—	Al	<.05T
			B	<.01
186	61.27	±0.1	Ba	<.02
			Ca	.1
187	3.31	0.05	Co	<.05
			Cr	<.05
188	9.54	0.1	Cu	.05
			Fe	.05
189	7.31	0.1	Ir	<.05
			K	<.01
190	8.77	0.1	Li	<.01
			Mg	<.05T
192	9.8	0.1	Mn	<.02
			Mo	<.02
			Na	<.01
			Ni	<.05
			Pb	<.05
			Pd	<.05
			Pt	<.05
			Rh	<.05
			Ru	<.05
			Si	.05
			Sn	<.05
			Ti	<.02
			V	<.02
			Zr	<.1

< —No spectrum line visible. Probably absent. Definitely less than value given.

<T —Present, but less than value given.

Table II. Composition Of Osmium Isotopes

Enriched In Mass Number 187

Isotopic Analysis			Spectrographic Analysis	
Isotope	Atomic %	Precision	Element	%
184	< 0.01	—	Al	.03
			B	.01
186	1.43	±0.05	Ba	<.02
			Ca	.03
187	45.76	0.1	Co	<.05
			Cr	<.05
188	25.74	0.1	Cu	.05
			Fe	.05
189	9.27	0.07	Ir	<.05
			K	<.01
190	9.38	0.07	Li	<.01
			Mg	<.02T
192	8.43	0.07	Mn	<.02
			Mo	<.05
			Na	<.01
			Ni	<.05
			Pb	<.1
			Pd	<.05
			Pt	<.05
			Rh	<.05
			Ru	<.05
			Si	.1
			Sn	<.05
			Sr	<.05
			Ti	<.02
			V	<.02
			Zr	<.1

< —No spectrum line visible. Probably absent. Definitely less than value given.

< T —Present, but less than value given.

Table III

Sample No.	Activity	Bombardment Off	Duration of Bombardment	Bombarding Particle	Sample Configuration
N1794	Os^{186}+p	9:30 Feb 2,'62	1/2 hour	6 mev p	Flat
N1795	Os^{186}+p	9:30 Feb 2,'62	1/2 hour	6 mev p	Well
N1796	Os^{187}+p	11:00 Feb 2,'62	1/2 hour	6 mev p	Flat
N1805	Os^{186}+p	13:40 Mar 9,'62	3/4 hour	6 mev p	Inverted target
N1845	Os^{186}+p	10:00 Jun 22,'62	1 hour	6 mev p	Well
N1847	Os^{186}+p	10:00 Jun 22,'62	1 hour	6 mev p	Flat

Other elements like Ca, Cu, Fe, and Si, small traces of which were found in the spectrographic analysis of O.R.N.L. (Table I), produced by (p,n) reaction some small activities from a few seconds to nearly four hours. Some of these activities are very short-lived strong positron emitters and visibly influenced (along with 3.2 h Ir^{190}) the 511 peak of the spectrum (figure 9). These activities produced no visible spectral peaks but influenced the early decay curves of Ir^{186} energy peaks. For the activities of these elements and that due to 3.2 h Ir^{190} we had to wait nearly 16 hours after bombardment before making any reasonably acceptable spectral analysis. In this context it may be mentioned that Fe and Cu impurities produced small traces of long-lived isotopes (77 to 264d) which were found to be present from three to four weeks after bombardment till as long as three months thereafter along with the 75 d activity of Ir^{192} (figure 21). These long-lived small activities along with others were taken care of in finding out the decay rate of energy peaks and unscrambling of gamma spectrum.

The immediate problem in spectral analysis was, however, the presence of 12 h Ir^{187} activity, though, of course, in a small percentage. To detect its influence on Os^{186}+p activity, i.e., in sample N1794, an osmium sample enriched in mass 187 (Table II) was bombarded with 6 mev proton and the two spectra Os^{186}+p and Os^{187}+p were compared with one another (figure 7 and figure 8). Later analysis of x-ray of Os^{187}+p showed a 12 h half-life clearly distinguished from 15 h half-life of x-ray observed in Os^{186}+p sample. The two spectra had no common

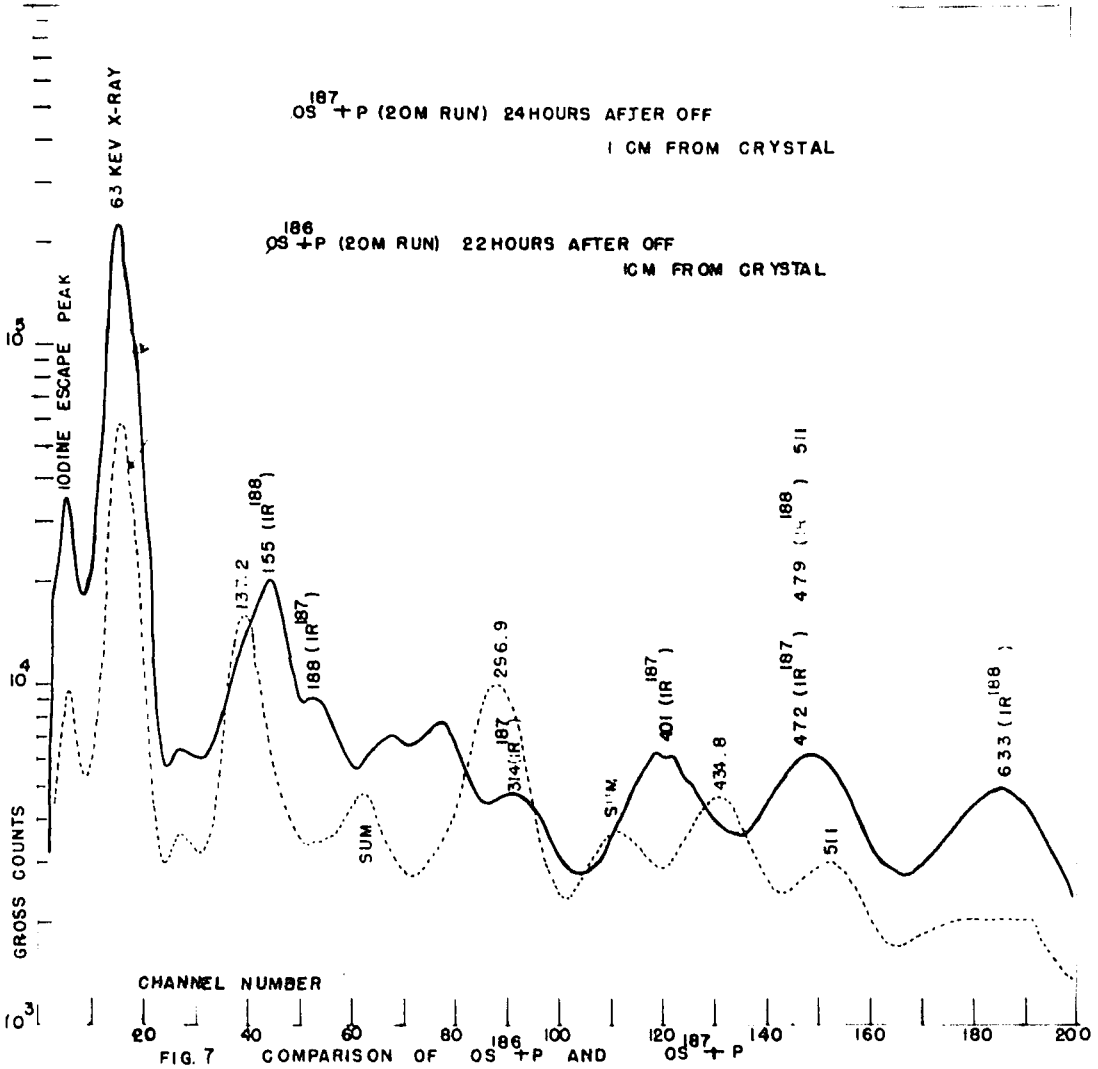

FIG. 7 COMPARISON OF OS^{186} + P AND OS^{187} + P

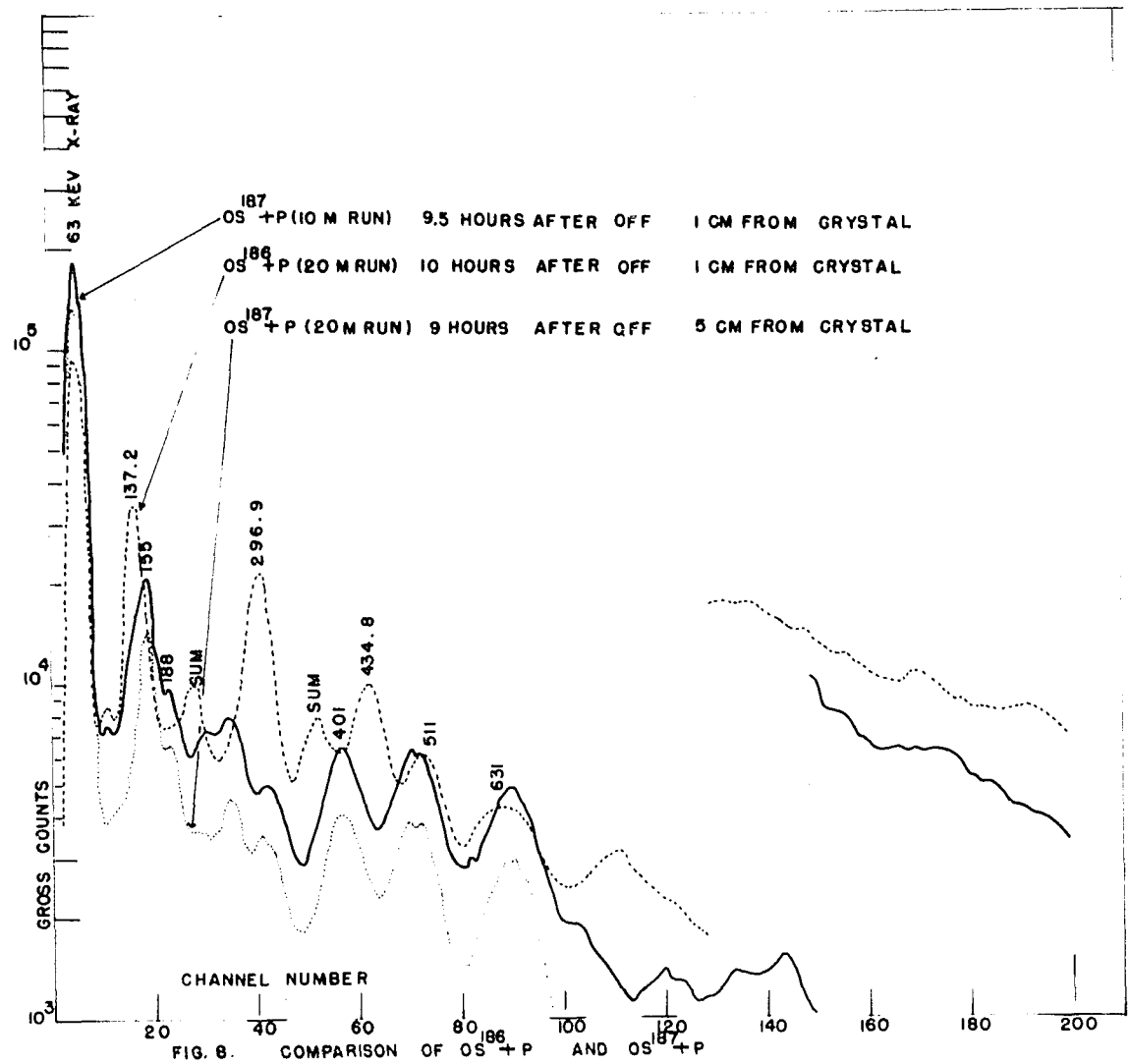

FIG. 8. COMPARISON OF OS^{186} + P AND OS^{187} + P

energy peaks and no line in Os^{186}+p produced a 12 h activity after peeling. Thus, it was concluded that the effect of Ir^{187} on the spectrum of Os^{186}+p was small and negligible.

In fact, the activity that influenced the decay of Ir^{186} most was that of 41 h Ir^{188}. Instead of trying to subtract one spectrum from another the effect of Ir^{188} was measured in course of the peeling off of decay curves and was properly subtracted from the unscrambled spectrum to produce correct intensity of Ir^{186} gamma rays. This will be discussed in detail later.

With the above discussion in mind it will be worthwhile, now, to make a comparative chronological study of the spectra obtained from proton bombardment of Os enriched in mass 186.

It has already been mentioned that all three different bombardments qualitatively followed identical patterns of decay. The best examples of spectra of all these three samples are collected together and explained in chronological order after bombardment.

Figure 9 shows a low gain spectrum of N1845 taken 22 minutes after bombardment. The spectrum has been taken with source at a distance of 6.5 cm from 3-inch x 3-inch crystal with minimum summing effect. Energy peaks shown are all of those of Ir^{186} decay—only, at particular places being highly modulated by short-lived activities as at 511 kev and 1.15 mev. Due to low gain, Os K x-ray of 63 kev is not visible. 435 kev of Ir^{186} has been completely shadowed by the annihilation radiation.

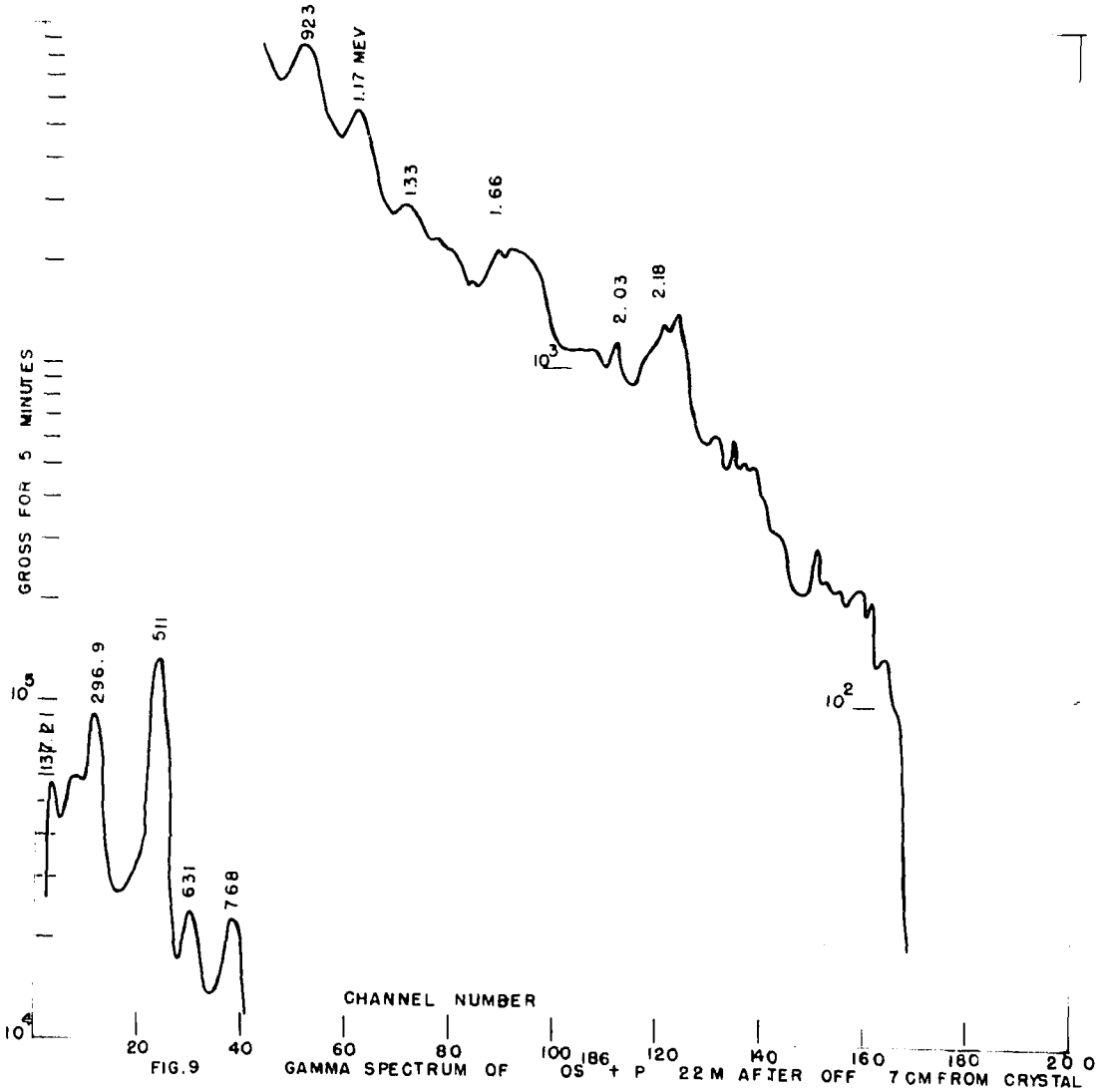

FIG. 9 GAMMA SPECTRUM OF ^{186}OS + P 22 M AFTER OFF 7 CM FROM CRYSTAL

Figures 10 and 11 show in-well and out-well spectra of N1795 at high gain with well crystal, one set taken two hours after off and the second set four hours after off. Besides 511+511 sum, two other sum peaks, one at 137+63 kev and the other at 297+63 kev, are visible. Strong summing at 137+63 suggests a strong coincidence of x-ray with 137 kev which finally was found to be a strong electron capture transition to 137 level.

Figure 12 shows two low gain spectra of N1845 taken 14 hours after off. One was taken with source at a distance 6.5 cm from the 3-inch x 3-inch crystal and the other at a distance of 0.5 cm. Since probability of coincidence summing is inversely proportional to the square of the solid angle subtended by the source to the front of the crystal[8], summing effects of 137+63 and 297+63 are very small in the former spectrum.

Figure 13 is the low gain spectrum of N1845 taken 19 hours after off with source at a distance of 6.5 cm from 3-inch x 3-inch crystal. All peaks belong to Ir^{186} decay with 631 kev and 1.66 mev mixed with an appreciable influence of 634 kev and 1.71 mev, respectively, of 41 h Ir^{188} decay.

Figure 14 shows two high gain spectra of N1794 taken 20 hours after off with source at a distance of 5 cm and 1 cm from 3-inch x 3-inch crystal. Summing effect due to change of solid angle as discussed earlier is also pronounced in this case.

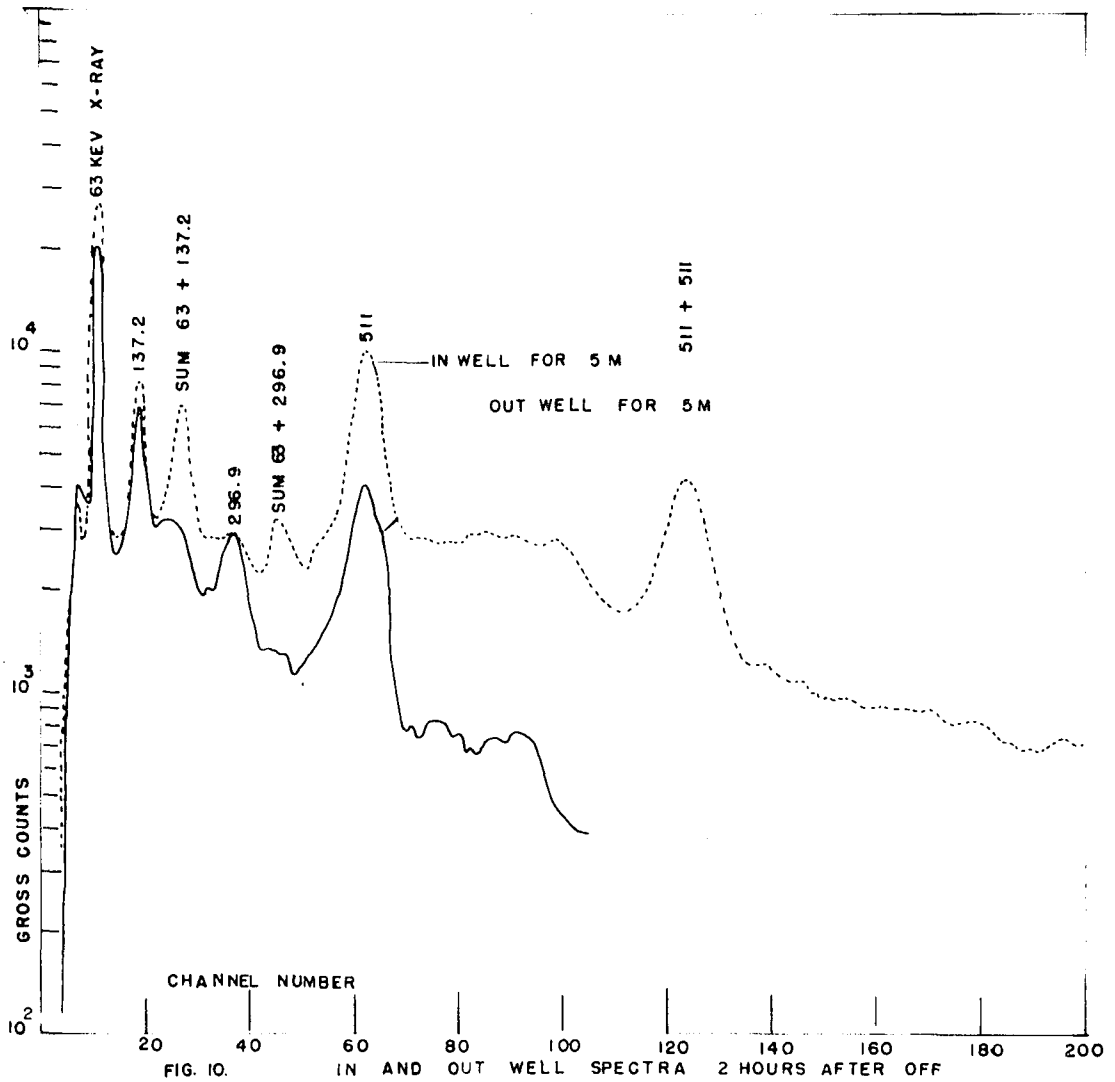

FIG. 10. IN AND OUT WELL SPECTRA 2 HOURS AFTER OFF

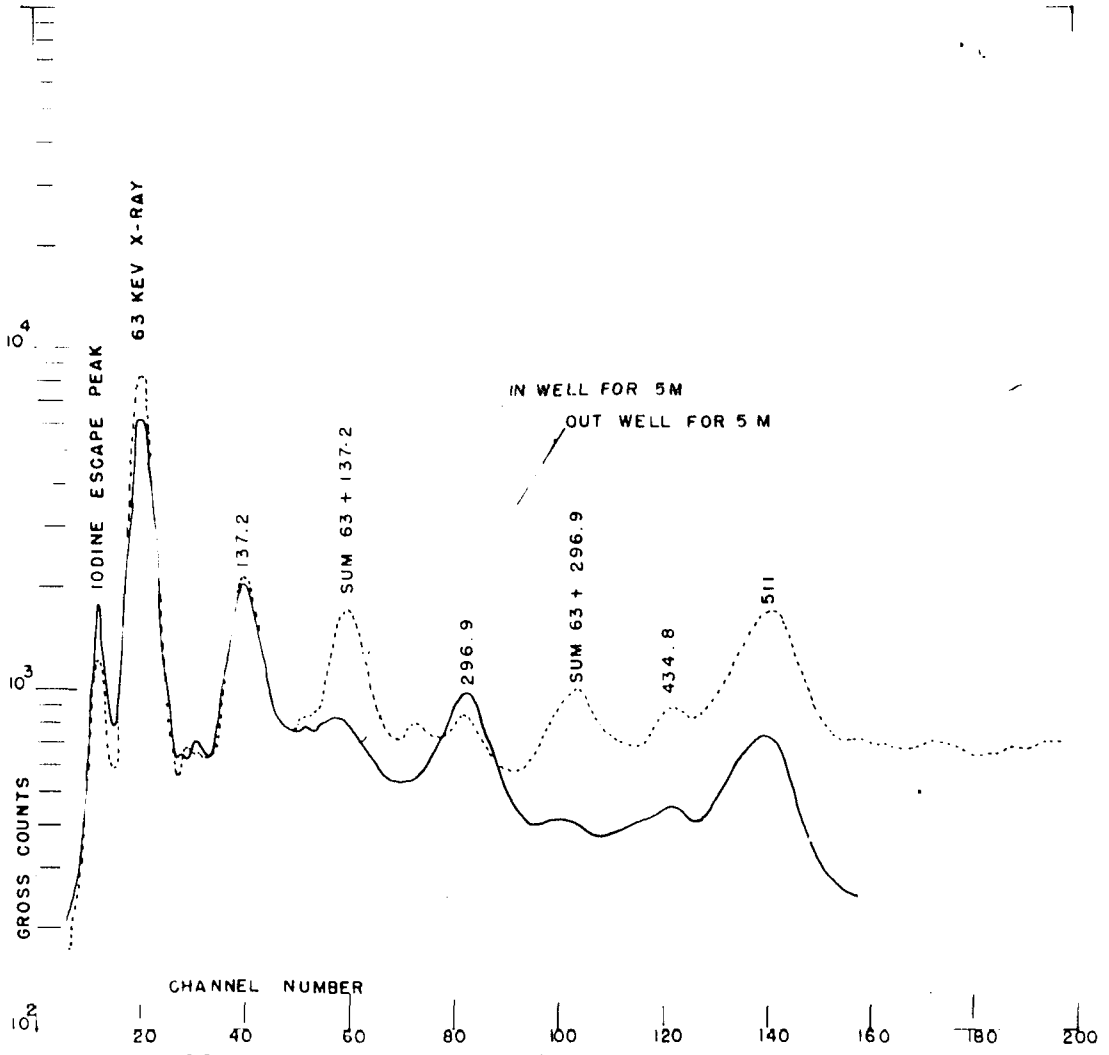

FIG. 11. IN AND OUT WELL SPECTRA 4 HOURS AFTER OFF

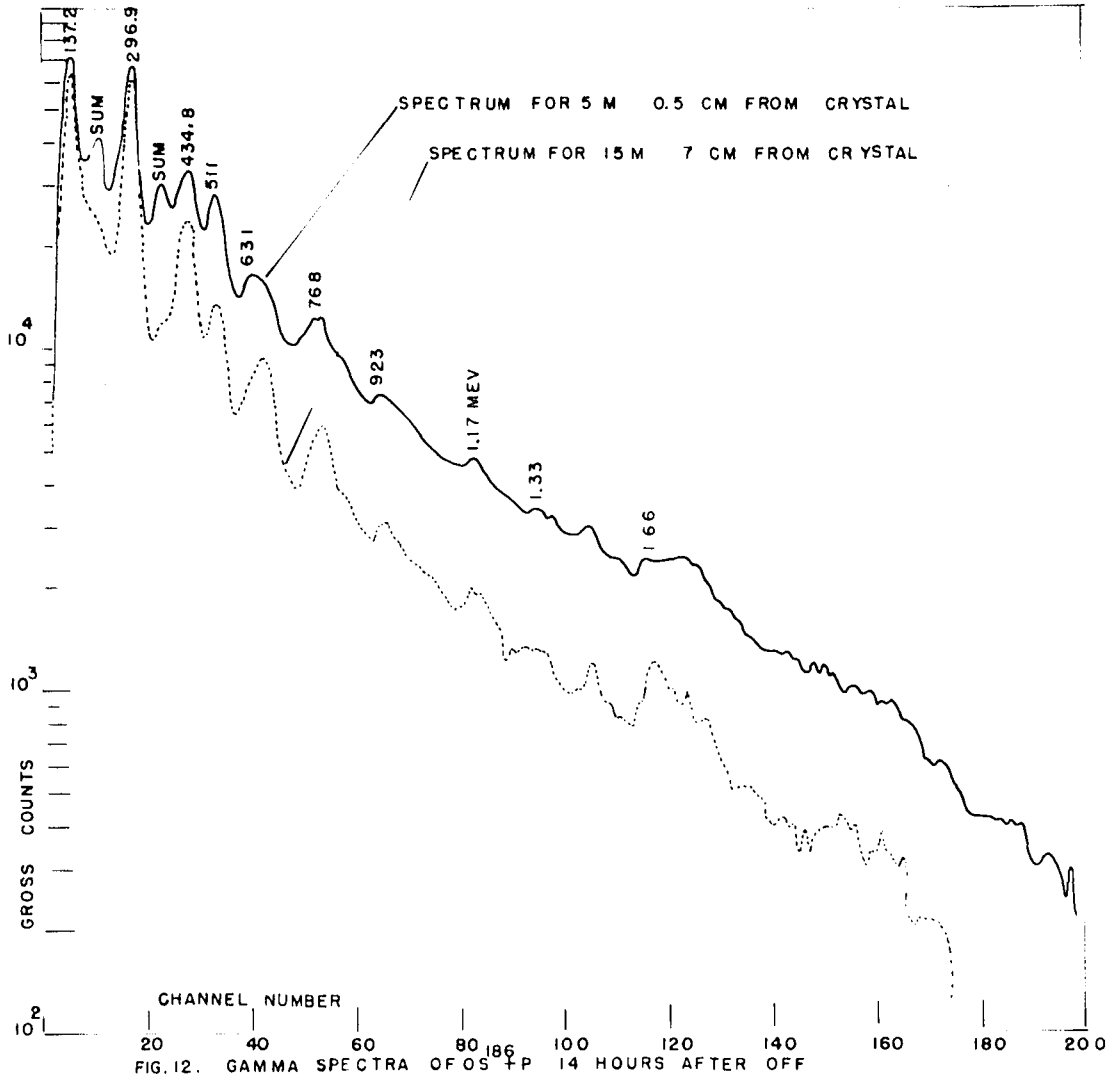

FIG. 12. GAMMA SPECTRA OF OS + P 14 HOURS AFTER OFF

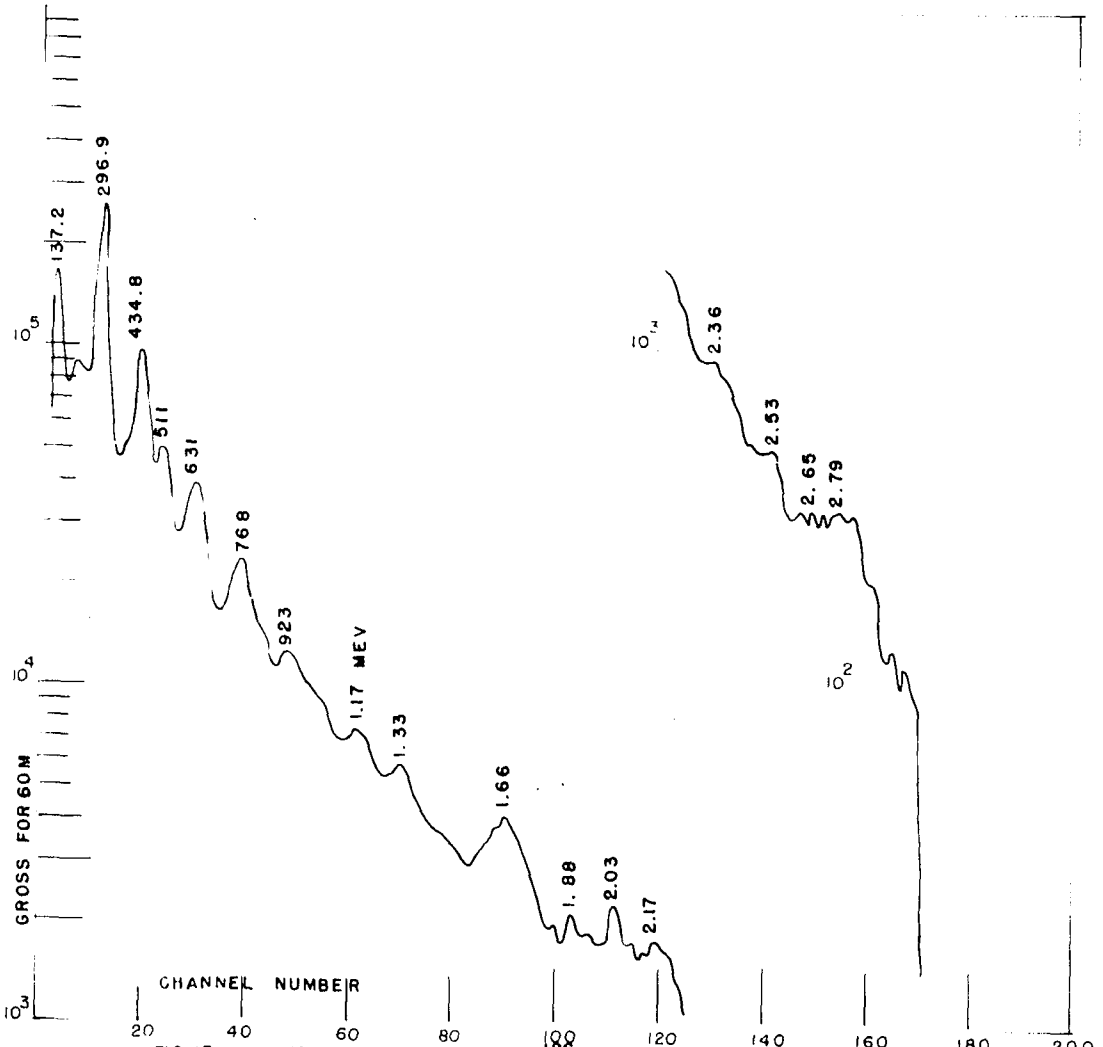

FIG. 13. GAMMA SPECTRUM OF $OS^{186}+P$ 19H AFTER OFF 7 CM FROM CRYSTAL

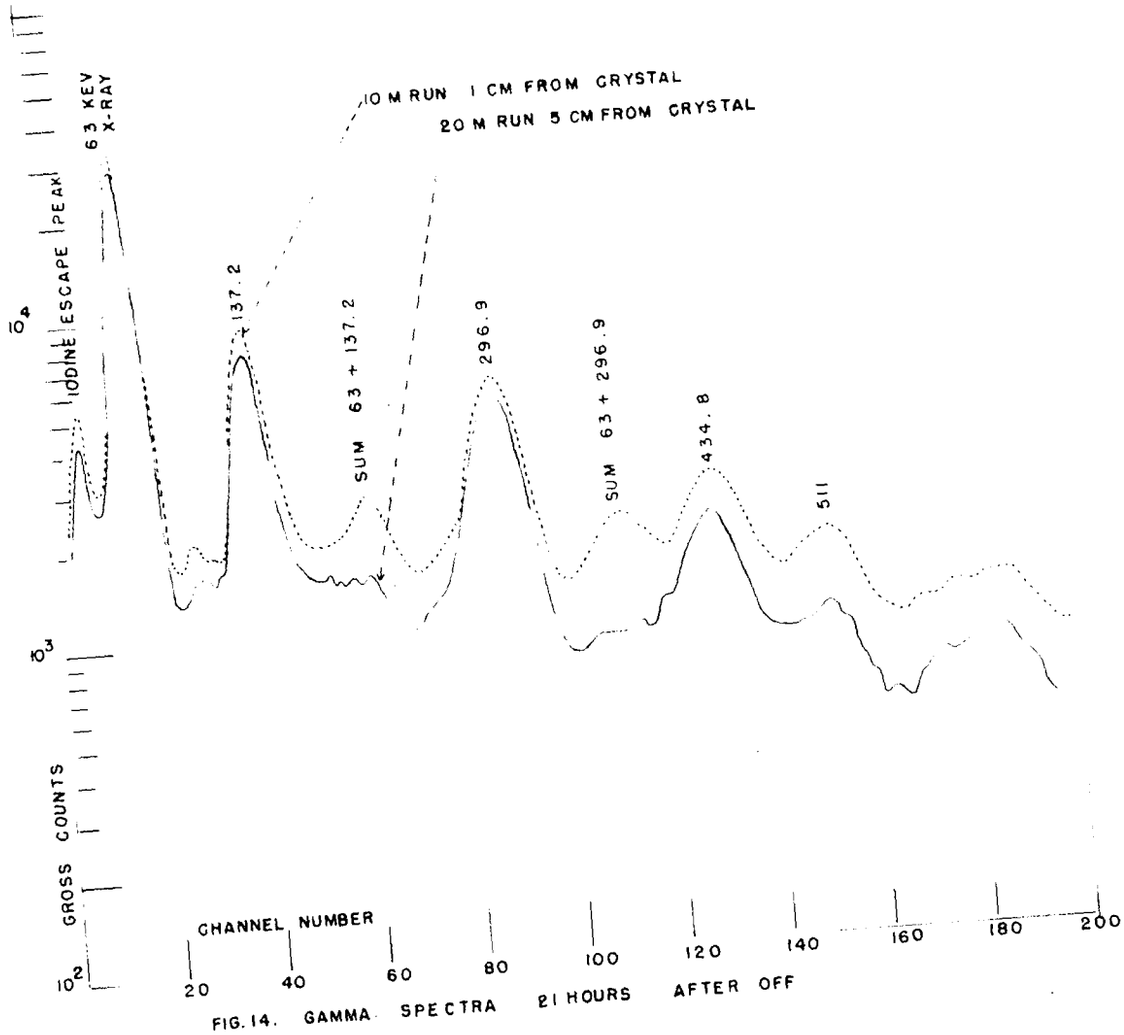

FIG. 14. GAMMA SPECTRA 21 HOURS AFTER OFF

Figure 15 shows two x-ray spectra of N1845 taken with x-ray scintillator 31 hours after off. The source was contained in a gelatine capsule to prevent L-absorption. The first spectrum was taken for 20 minutes without any absorber and the second spectrum was taken for the same length of time with an aluminium absorber of 172 mgm/cm^2. In the second case L x-ray was totally absorbed leaving K x-ray and its iodine escape peak only little affected. From this experiment an approximate estimate of L x-ray was obtained.

Figures 16, 17 and 18 are spectra of N1805 taken at different gains six days after bombardment. Spectrum of Ir^{186} completely disappeared with spectra of 41 h Ir^{188}, 11 d Ir^{189}, 11 d Ir^{190} and 75 d Ir^{192} becoming gradually prominent.

Figure 19 shows disappearance of 41 h Ir^{188} and gradual prominence of 75 d Ir^{192}, 10 days after off.

Figure 20 shows gradual disappearance of 11 d Ir^{189} and 11 d Ir^{190} after 43 days with prominence of 75 d Ir^{192}, 77 d Co^{56} and 245 d Zn^{65}, the latter two being produced from Fe and Cu impurities.

Figure 21 taken 95 days after off shows only long-life activities of Ir^{192}, Co^{56} and Zn^{65}.

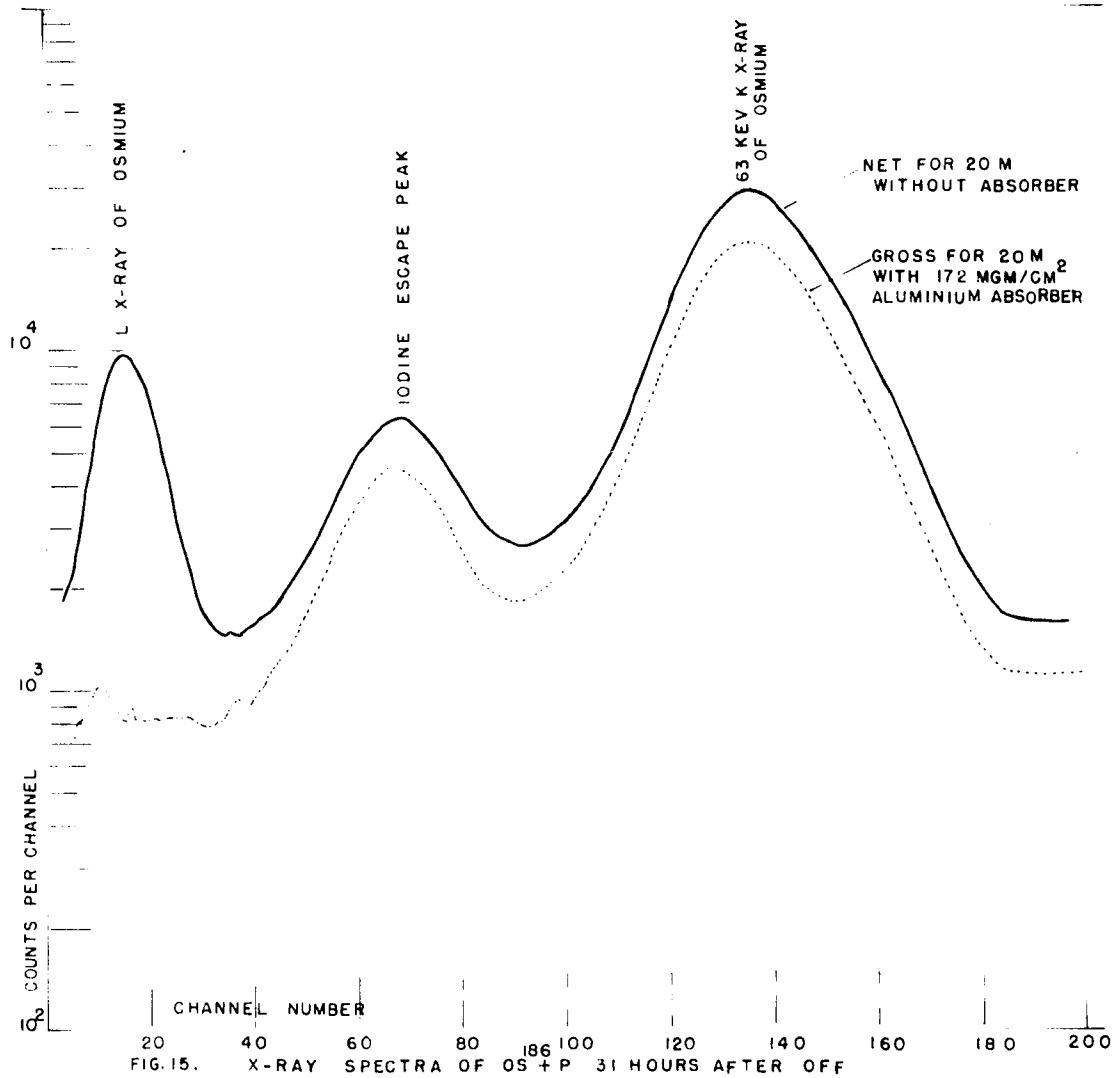

FIG. 15. X-RAY SPECTRA OF OS + P 31 HOURS AFTER OFF

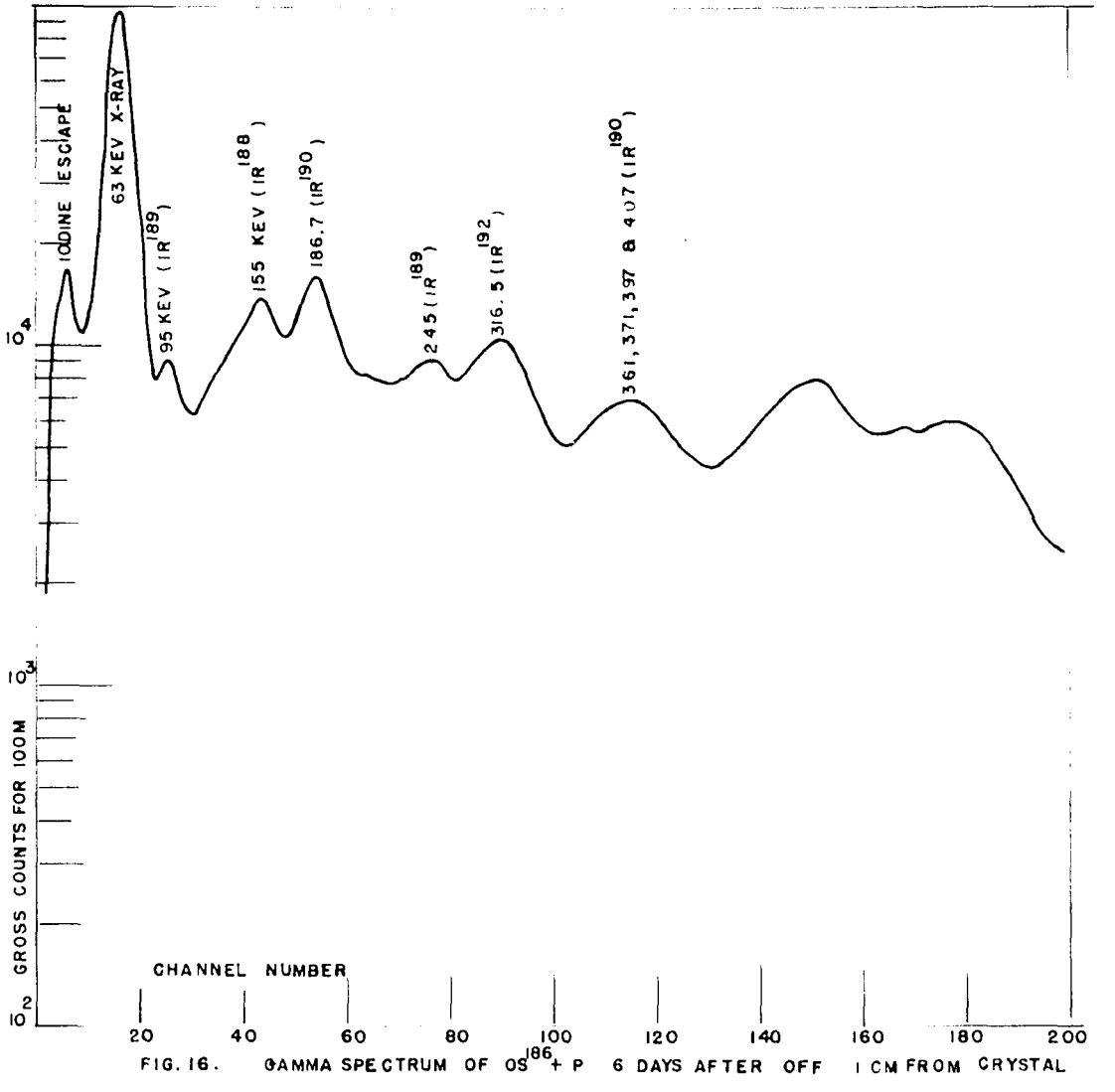

FIG. 16. GAMMA SPECTRUM OF Os^{186} + P 6 DAYS AFTER OFF 1 CM FROM CRYSTAL

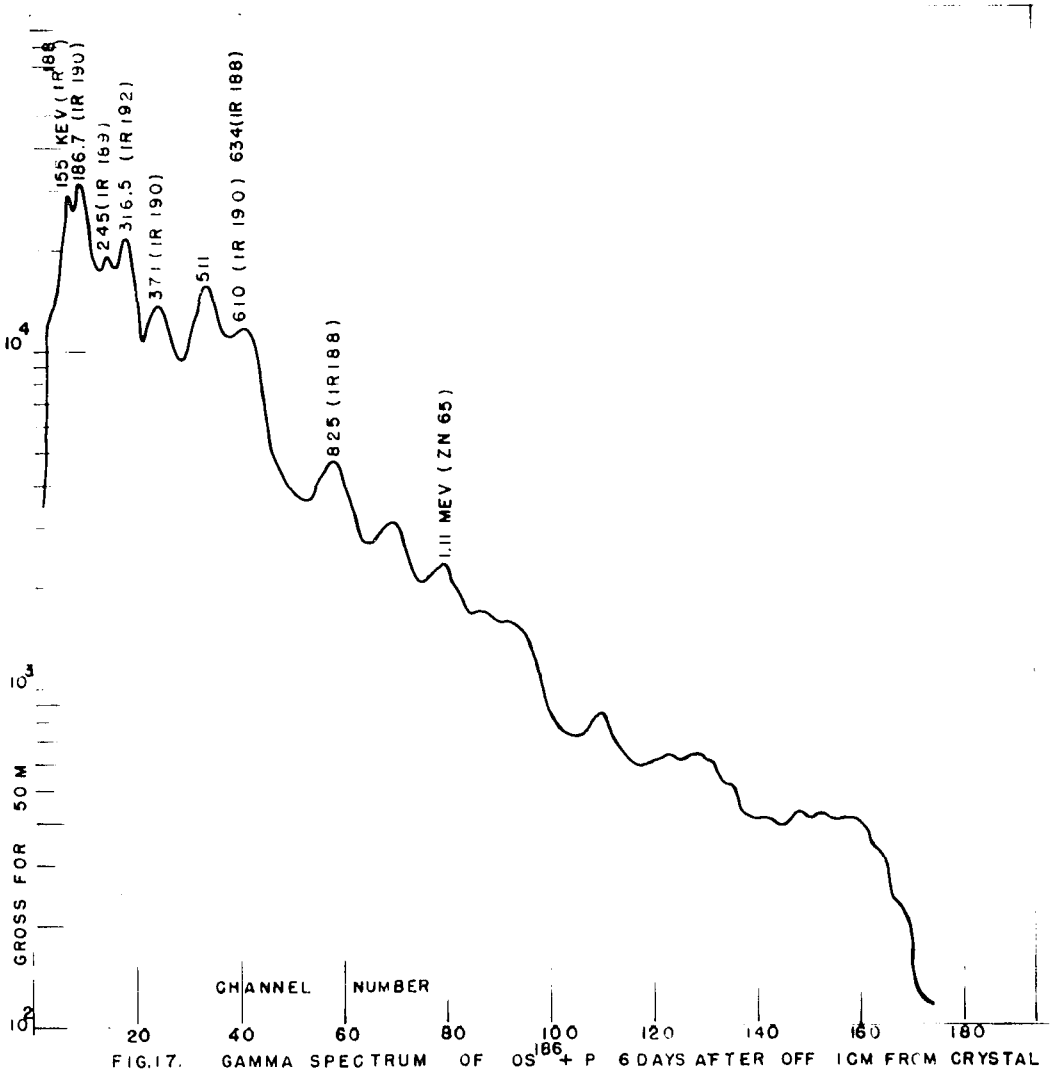

FIG. 17. GAMMA SPECTRUM OF OS^{186} + P 6 DAYS AFTER OFF 1CM FROM CRYSTAL

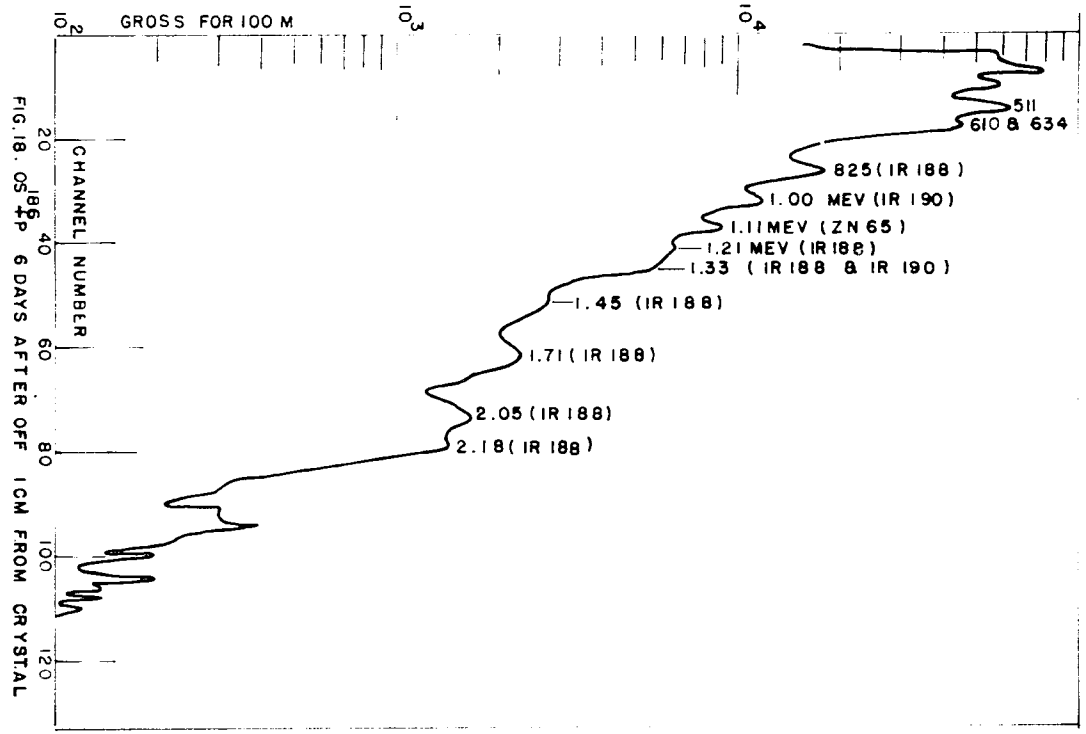

FIG. 18. OS^{186}P 6 DAYS AFTER OFF ICM FROM CRYSTAL

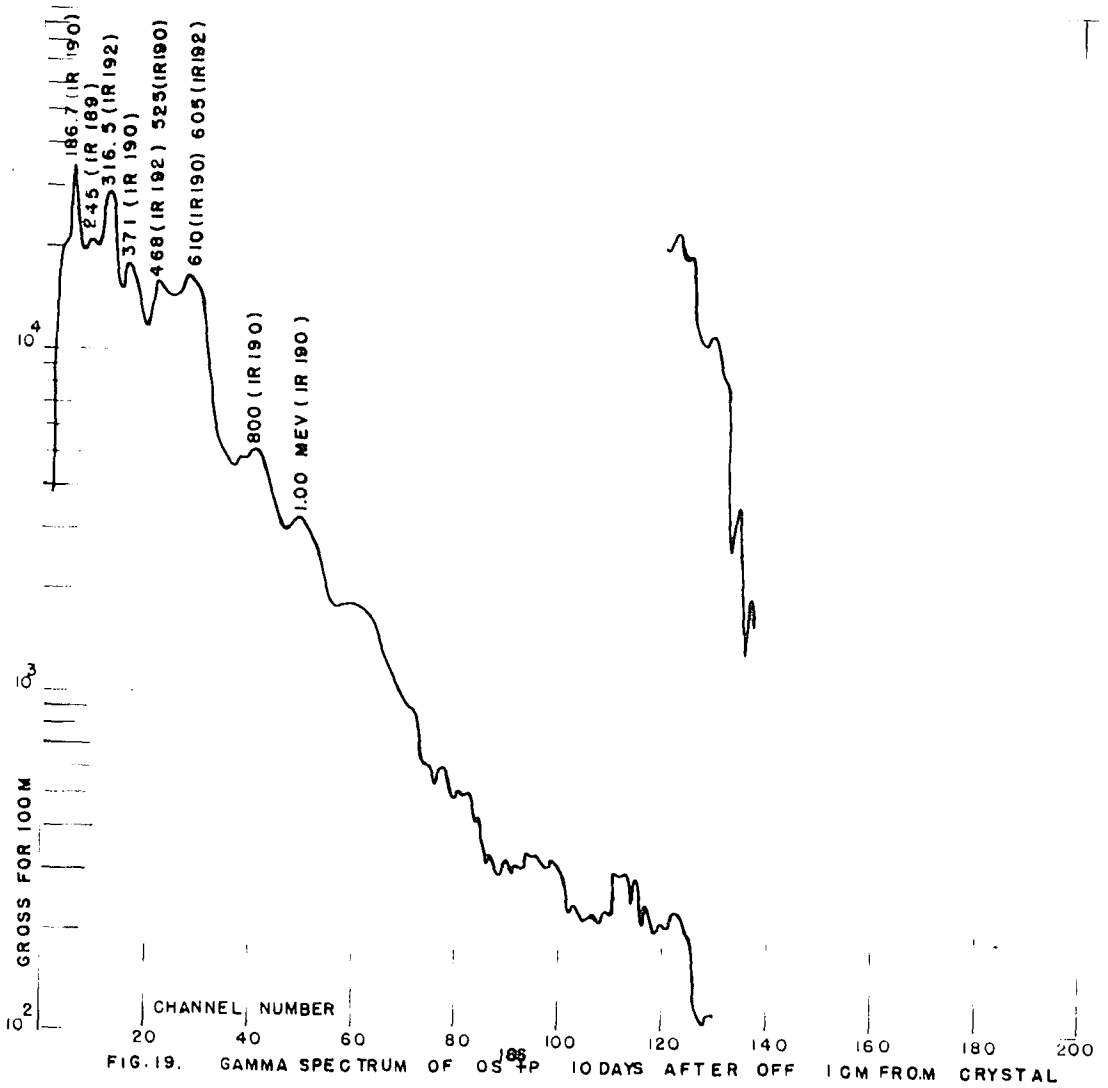

FIG. 19. GAMMA SPECTRUM OF ^{185}OS + P 10 DAYS AFTER OFF 1 CM FROM CRYSTAL

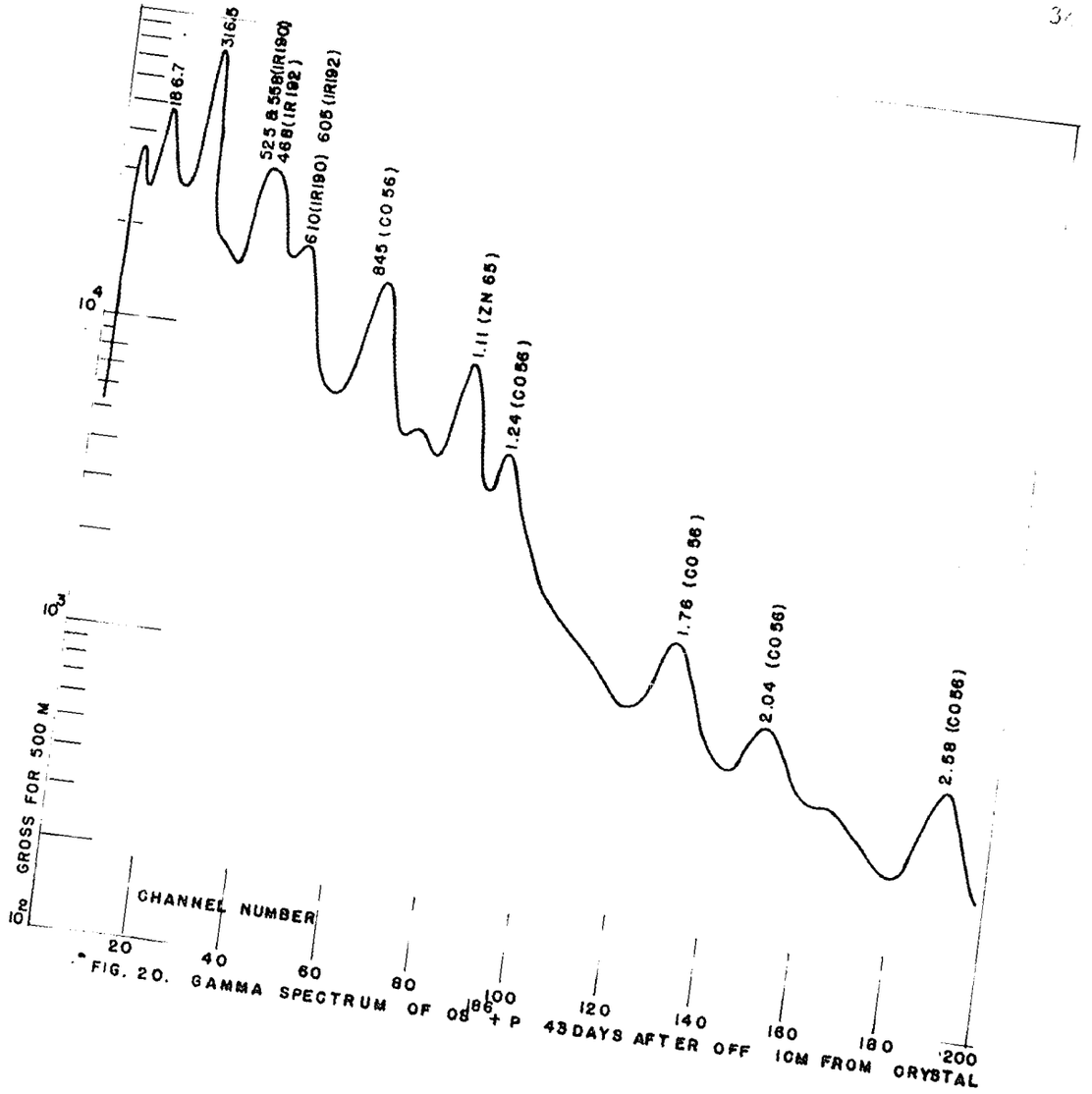

FIG. 20. GAMMA SPECTRUM OF 08

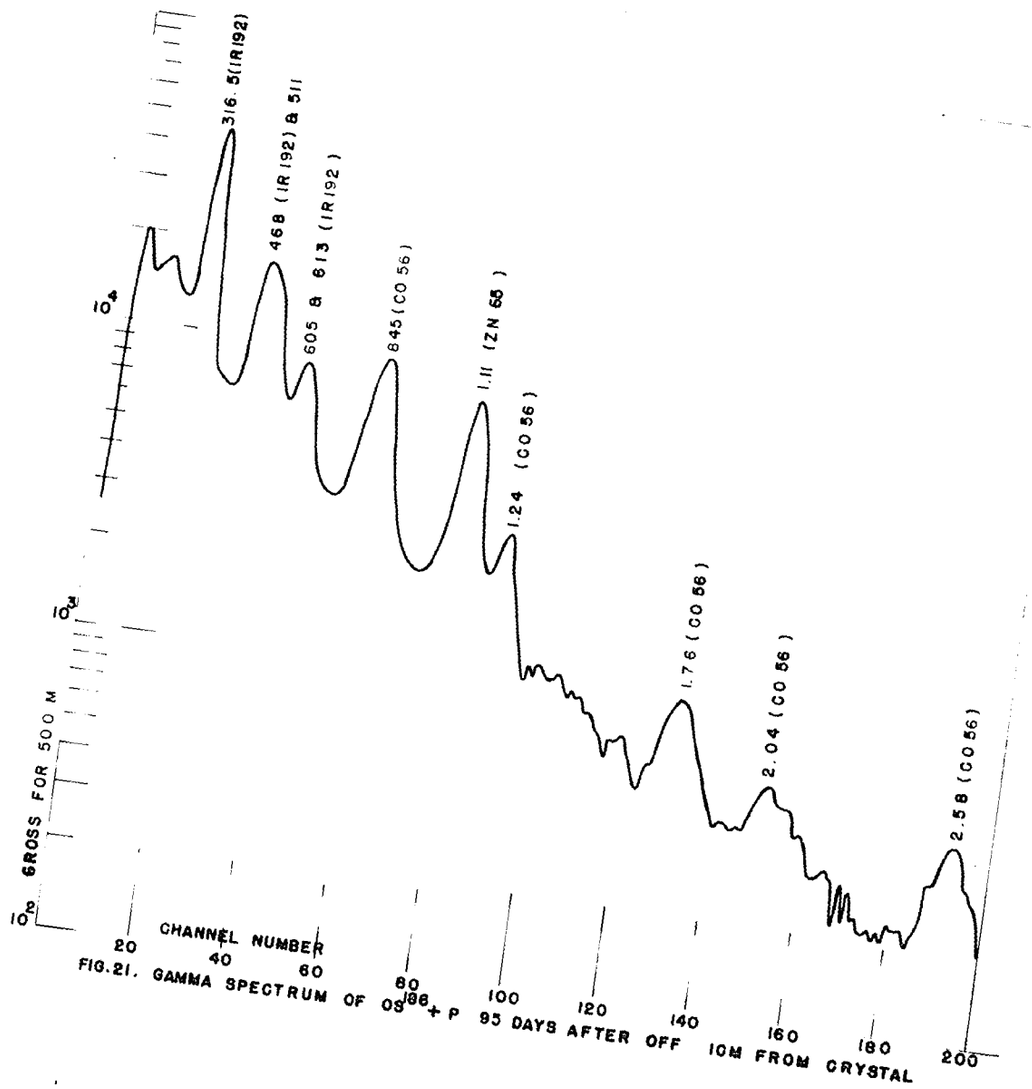

FIG.21. GAMMA SPECTRUM OF ^{186}OS + P 95 DAYS AFTER OFF 10M FROM CRYSTAL

(b) Rate Of Decay And Half-Life

As already mentioned, for a few hours immediately after bombardment decay curves of the energy peaks demonstrated a number of very short-lived activities of the order of a few minutes to nearly four hours which were due to impurities and 3.2 hours Ir^{190} isomer. After nearly 8 to 10 hours since the bombardment, the curves exhibited a steady decay, which eventually was found to be of 15 hours. After two to three days, decay rates were subsequently influenced by 41 h Ir^{188}, 11 d Ir^{189}, 11 d Ir^{190}, 75 d Ir^{192}, 77 d Co^{56} and 245 d Zn^{65}. Decay curves of each energy peak were carefully peeled off and the observed activity in the 15 h region gave the results which are reproduced in Table IV. Figure 22 shows the nature of decay of different energy peaks. In assigning energy peaks to 15 h Ir^{186} activity much care was taken to study the relative contribution of 15 h, 41 h, 11 d, 75 d, etc., activities in the peeled off decay curves. In the decay of energies ascribed to the activity of Ir^{186} the contribution due to 41 h, 11 h, etc. activities were by far less than that of 15 h and, thus, the latter could not be regarded as only compton distribution effect of higher energies. Activities at 2.55 mev, 2.65 mev and 2.79 mev demonstrated almost a single moderately strong activity of 15 h.

Table IV. Half Lives of Energy Peaks

Energy		Half life
63	kev x-ray	14.2 h
137.2	kev	15.5 h
296.9	kev	15.7 h
434.8	kev	14.9 h
511	kev	14.8 h
631	kev	14.8 h
768	kev	15.7 h
923	kev	14.0 h
1.17	mev	14.4 h
1.33	mev	14.9 h
1.66	mev	14.9 h
2.03	mev	14.4 h
2.17	mev	14.7 h
2.36	mev	15.0 h
2.53	mev	15.0 h
2.65	mev	15.0 h
2.79	mev	15.0 h

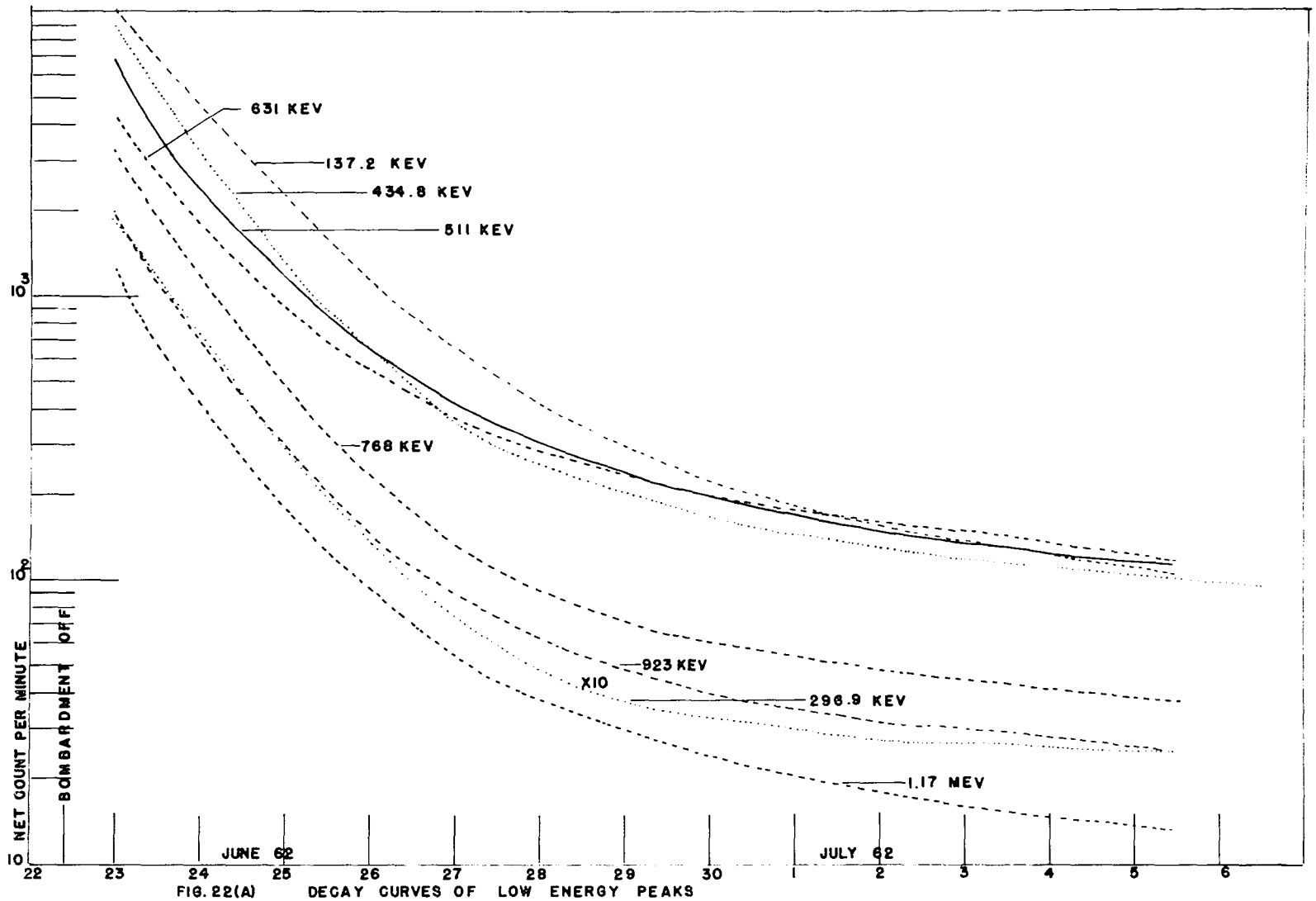

FIG. 22(A) DECAY CURVES OF LOW ENERGY PEAKS

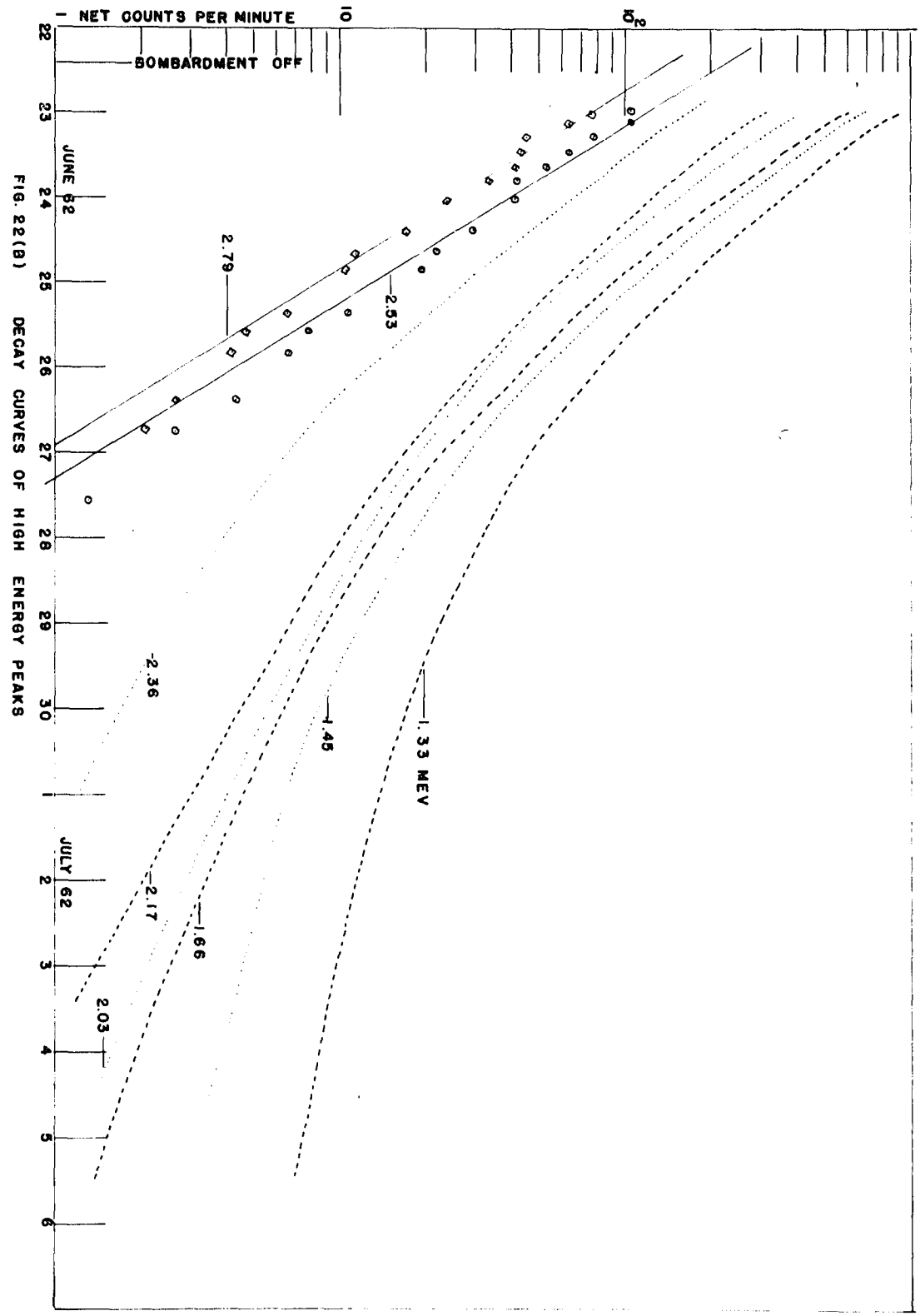

FIG. 22(B) DECAY CURVES OF HIGH ENERGY PEAKS

Unscrambling Of Spectrum And Transition Probabilities

To determine the relative intensities of the energy peaks of Ir^{186} and from them the relative transition probabilities of Ir^{186} gamma rays unscrambling of a suitable gamma spectrum was carried on as suggested and detailed in different references.[8,9,10]

In a gamma ray spectrum obtained by a 3-inch x 3-inch NaI(Tl activated) crystal energies at different ranges demonstrate three distinctly different kinds of pulse-height distribution. Energies near 137.2 kev show a distinct iodine escape peak far above the compton distribution. Energies beyond this up to nearly 1.02 mev show a prominent distribution of compton scattered photons. Energies beyond 1.02 mev start producing electron positron pairs and in the region of 2 mev gamma rays, in addition to the photo-peak, single and double escape peaks[8] become very prominent. In order to emphasize this characteristic pulse-height distribution a number of standard sources were prepared by neutron bombardment from O.S.U. research reactor. A list of the energy peaks and the corresponding standards taken to unscramble them is given in Table V.

Two spectra (figures 23 and 24) each nearly 20 hours after bombardment, one taken at a high gain and the other at a low gain, were carefully selected when the 15-hour activity was overwhelmingly predominant.

It is relevent to mention here that both of these unscrambled spectra were taken at a considerable distance from the crystal. In the case of low gain spectrum, the source-crystal distance was 7 cm and

in the case of high-gain spectrum this was 5 cm. This precaution was taken to reduce the effect of coincidence summing.

Table V

	Peak Unscrambled		Standard Peak Taken
High Gain	63	kev	
	137.2	kev	122 kev of Co^{57}
	296.9	kev	323 kev of Cr^{51}
	434.8	kev	323 kev of Cr^{51}
	511	kev	662 kev of Cs^{137}
Low Gain	434.8	kev	323 kev of Cr^{51}
	511	kev	662 kev of Cs^{137}
	631	kev	662 kev of Cs^{137}
	768	kev	835 kev of Mn^{54}
	923	kev	835 kev of Mn^{54}
	1.17	mev	1.119 mev of Zn^{65}
	1.33	mev	1.119 mev of Zn^{65}
	1.66	mev	1.52 mev of K^{42}
	2.03	mev	1.52 mev of K^{42}
	2.17	mev	2.76 mev of Na^{24}
	2.36	mev	2.76 mev of Na^{24}
	2.53	mev	2.76 mev of Na^{24}
	2.65	mev	2.76 mev of Na^{24}
	2.79	mev	2.76 mev of Na^{24}

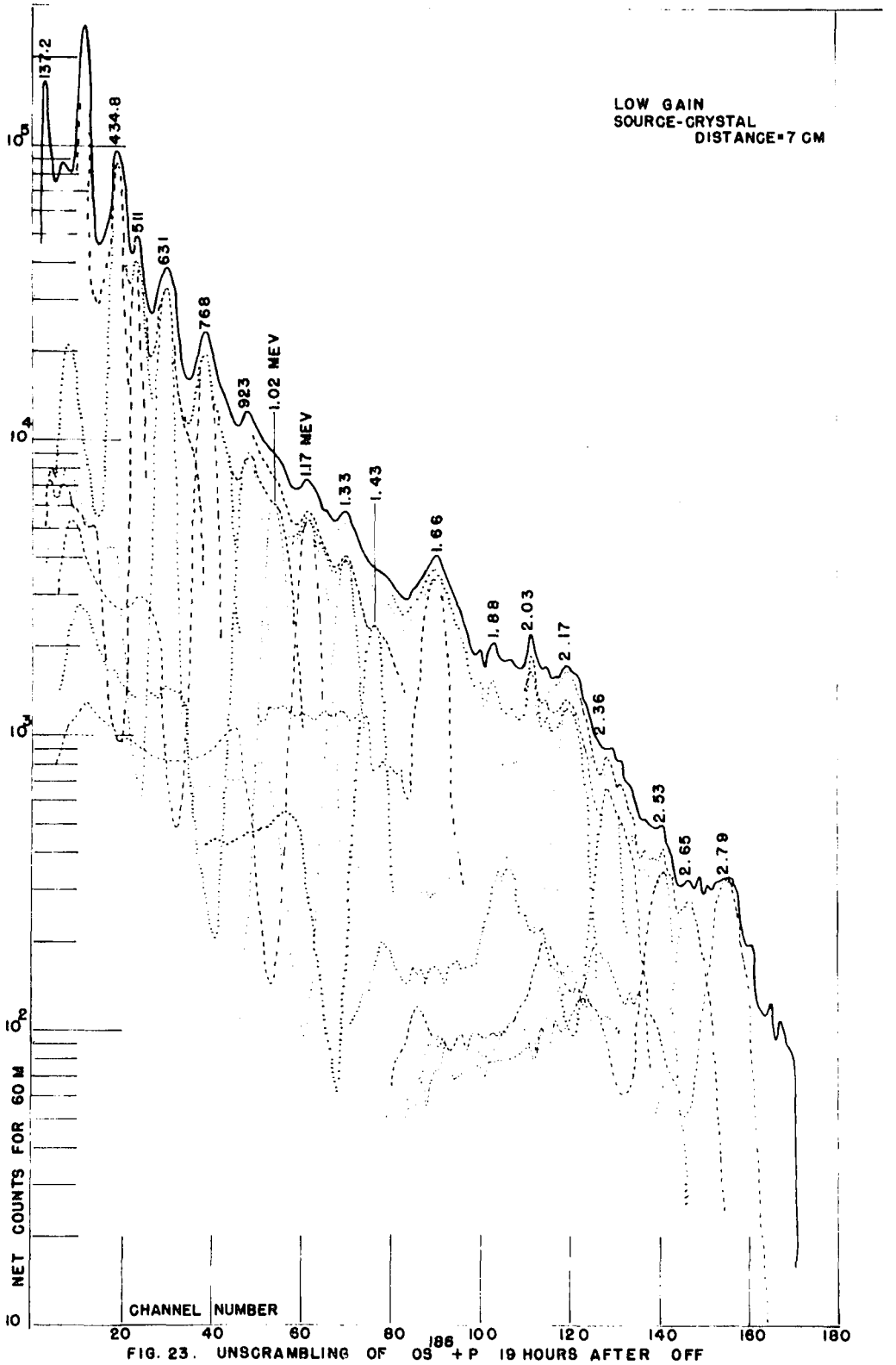

FIG. 23. UNSCRAMBLING OF ^{08} + P 19 HOURS AFTER OFF

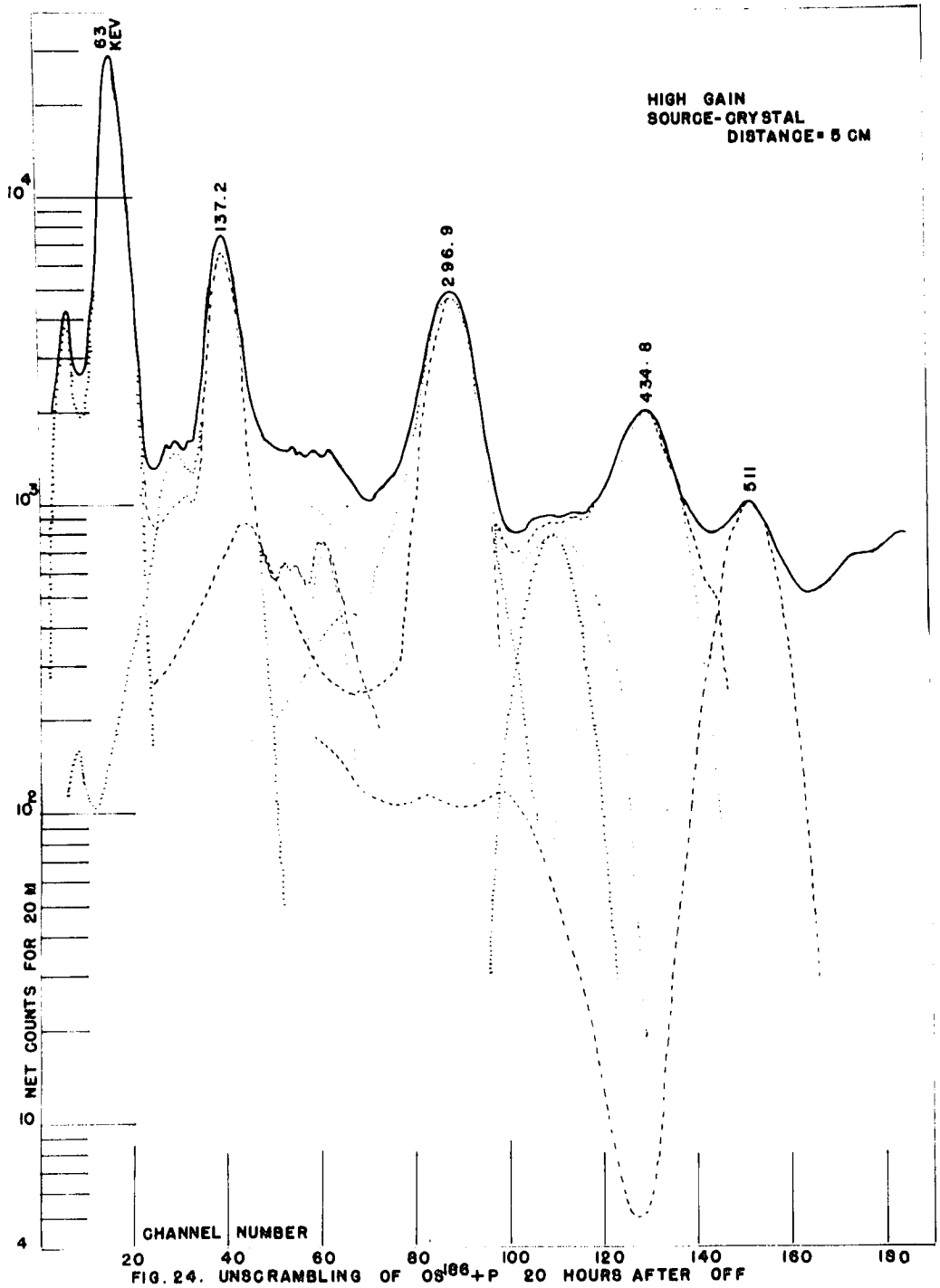

FIG. 24. UNSCRAMBLING OF Os^{186}+P 20 HOURS AFTER OFF

As a starting point in the process of unscrambling, 2.76 mev spectrum of Na^{24} was obtained by 3-inch x 3-inch crystal with the standard source in an identical geometry as that of the unknown one and the gain was so adjusted that 2.76 mev fell right on the channel corresponding to that of 2.79 mev of Ir^{186}. The photo-peaks were compared and standardized and then 2.76 mev spectrum with proper correction[10] for compton distribution, etc., was subtracted from the spectrum of Ir^{186}. This method of subtraction was continued for the rest of the spectrum and for both high-and low-gain spectra.

The number of counts, N_p, under each photo-peak was then measured. Considering energy of the peak and geometry of the source, absolute efficiency, ϵ, of the 3-inch x 3-inch crystal as well as peak-to-total ratio σ were found from ref. 8. Total count N_t corresponding to each energy was found by applying the formula,

$$N_t = N_p/\epsilon\sigma$$

From the unpeeled decay curve of the corresponding energy fractional contribution of 15 h Ir^{186} at the time of unscrambling was found and N_t was multiplied by that fraction to make an approximate elimination of other activities. The resultant count was the contribution due to corresponding energy of Ir^{186} activity.

Next correction necessary was that due to internal conversion electrons, which were, of course, necessary only for the low energy transitions, 137.2 kev, 296.9 kev, and 434.8 kev. These transitions

have already been established[4] as E2 transitions. Corresponding to Z=76 and for E2 transitions conversion coefficients a_k, a_{li}, a_{lii}, a_{liii}, a_{mi}, a_{mii}, a_{miii}, a_{miv}, and a_{mv} were tabulated from ref. 11 and plotted in figure 25. From figure 25 conversion coefficients corresponding to energies 137.2, 296.9, and 434.8 kev were obtained as shown in Table VI.

TABLE VI

Conversion Coefficients For E2 Transitions (Z=76)

E Energy in Mev	K =E/0.511	α_K	α_{Li}	α_{Lii}	α_{Liii}	α_{Mi}	α_{Mii}	α_{Miii}	α_{Miv}	α_{Mv}	$\alpha = \Sigma_i \alpha_i$
0.1372	0.268	4.0×10^{-1}	4.73×10^{-2}	3.15×10^{-1}	2.57×10^{-1}	1.8×10^{-2}	1.38×10^{-1}	1.12×10^{-1}	1.97×10^{-3}	1.48×10^{-3}	1.2903
0.2969	0.581	6.2×10^{-2}	7.9×10^{-3}	1.18×10^{-2}	6.6×10^{-3}	2.65×10^{-3}	5.0×10^{-3}	2.85×10^{-5}	4.4×10^{-5}	3.1×10^{-5}	0.100
0.4348	0.851	2.37×10^{-2}	3.2×10^{-3}	2.45×10^{-3}	1.13×10^{-3}	1.10×10^{-3}	1.13×10^{-3}	5.3×10^{-4}	7.4×10^{-6}	5.0×10^{-6}	0.033

Total K-Conversion Electrons = 31×10^4

Fluorescent Yield in K Shell (for Z=76) =0.948

Number of K-Capture= $(136-31)/0.948 \times 10^4 = 111 \times 10^4$

Number of K-electrons produced by conversion of these gamma rays was calculated and subtracted from x-ray intensity. This corrected intensity of x-ray was then divided by fluorescence yield obtained from ref. 12 to account for the auger electrons. Further, an approximate estimate of L-electrons was obtained by analysing figure 15 and added to the x-ray intensity. This, however, was a small fraction of the total.

A tabulation of the intensities is given in Table VII.

TABLE VII

Relative Transition Probabilities of Gamma Rays

E Energy in Mev	N_γ Number of Gamma Observed $\times 10^4$	α	$1+\alpha$	Number of K-Conversion Electrons $\times 10^4$	N_t =Total Number of Transitions $=N_e+N_\gamma=N_\gamma(1+\alpha)$ $\times 10^4$
0.063	136	-	-	-	111*
0.1372	63.4	1,290	2.290	25	145
0.2969	85.5	0.100	1.100	5	94
0.4348	60.8	0.033	1.033	1.4	63
0.511	26.5				26.5
0.631	28.1				28.1
0.768	28.6				28.6
0.923	16.2				16.2
1.17	13.9				13.9
1.33	12.0				12.0
1.66	16.0				16.0
2.03	6				6
2.17	6.3				6.3
2.36	4.8				4.8
2.53	3.7				3.7
2.65	3.4				3.4
2.79	3.9				3.9

*See bottom of Table VI

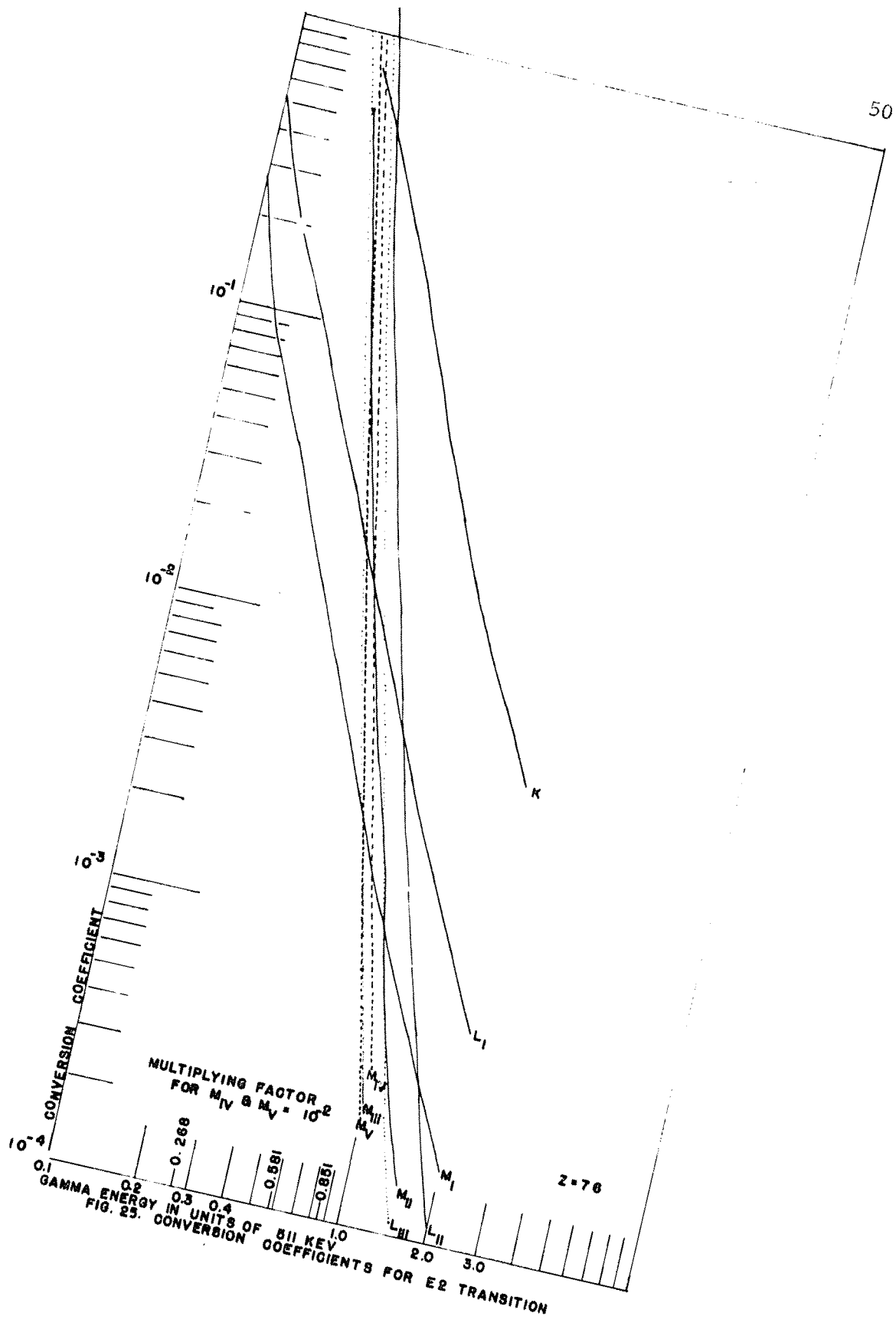

FIG. 25. CONVERSION COEFFICIENTS FOR E2 TRANSITION

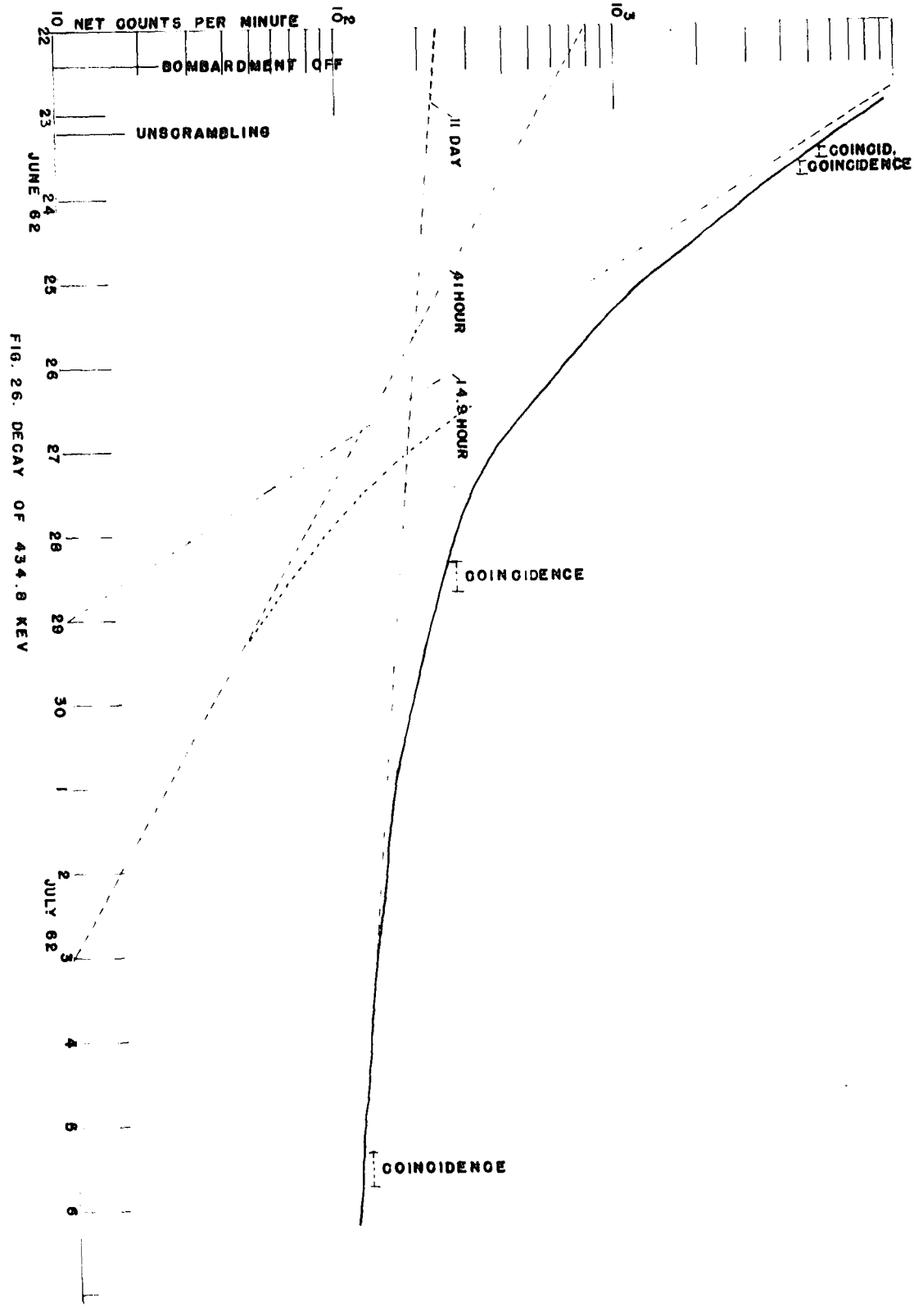

FIG. 26. DECAY OF 434.8 KEV

Coincidence Measurements

Gamma-gamma coincidence measurements were carried by a four-channel fast coincidence circuit and a 400-channel pulse-height analyser, each 100 channels of which produced response to one coincidence gate. Gamma source was sandwiched between two pieces of cardboard provided with thin mylar windows. This type of sample has been referred to as flat sample. This flat sample was placed in a compton shield to reduce effect of compton scattering. Coincidence heads were two 1 3/4-inch x 2-inch NaI (Tl) crystals facing each other at 180^{o}. The resolving power of these crystals is much lower than that of 3-inch x 3-inch crystal. Hence, the coincidences with gates at high energy peaks were doubtful and are not reproduced in this work.

Coincidence spectra with gates at 63 kev x-ray, 137.2 kev, 296.9 kev, 434.8 kev, 511 kev, 631 kev, 768 kev, and 923 kev were taken very carefully several times and at different regions of the decay curve. Figure 26 shows an example of it.

By comparing coincidence spectra taken at different periods, a qualitative estimate was made for the influence of activities other than that of 15 h Ir^{186}. This knowledge was used to find the true coincidence of the energy transitions of Ir^{186}. Figures 27, 28 and 29 are examples of the coincidence spectra observed and Table VIII shows the inferences drawn.

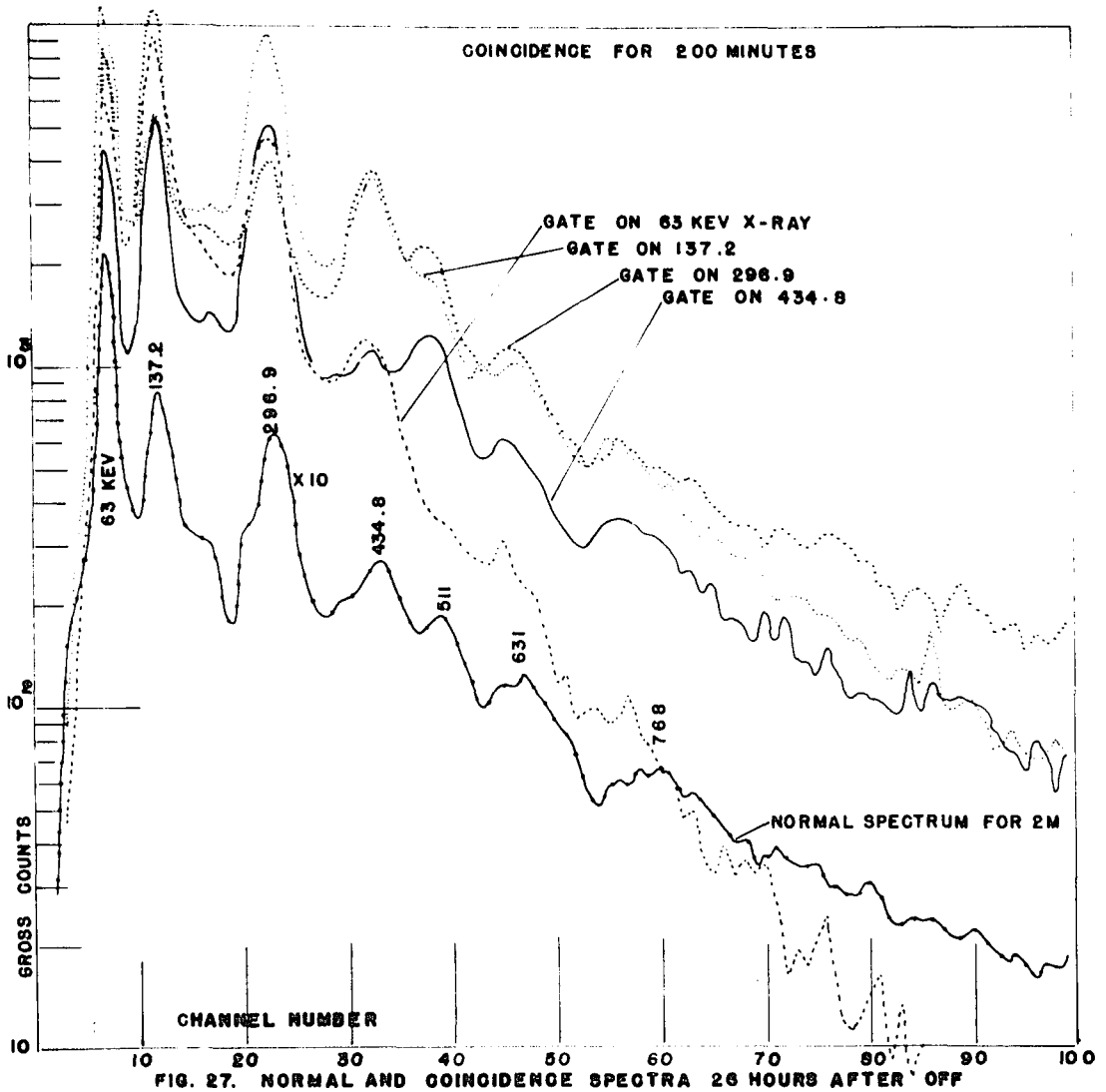

FIG. 27. NORMAL AND COINCIDENCE SPECTRA 26 HOURS AFTER OFF

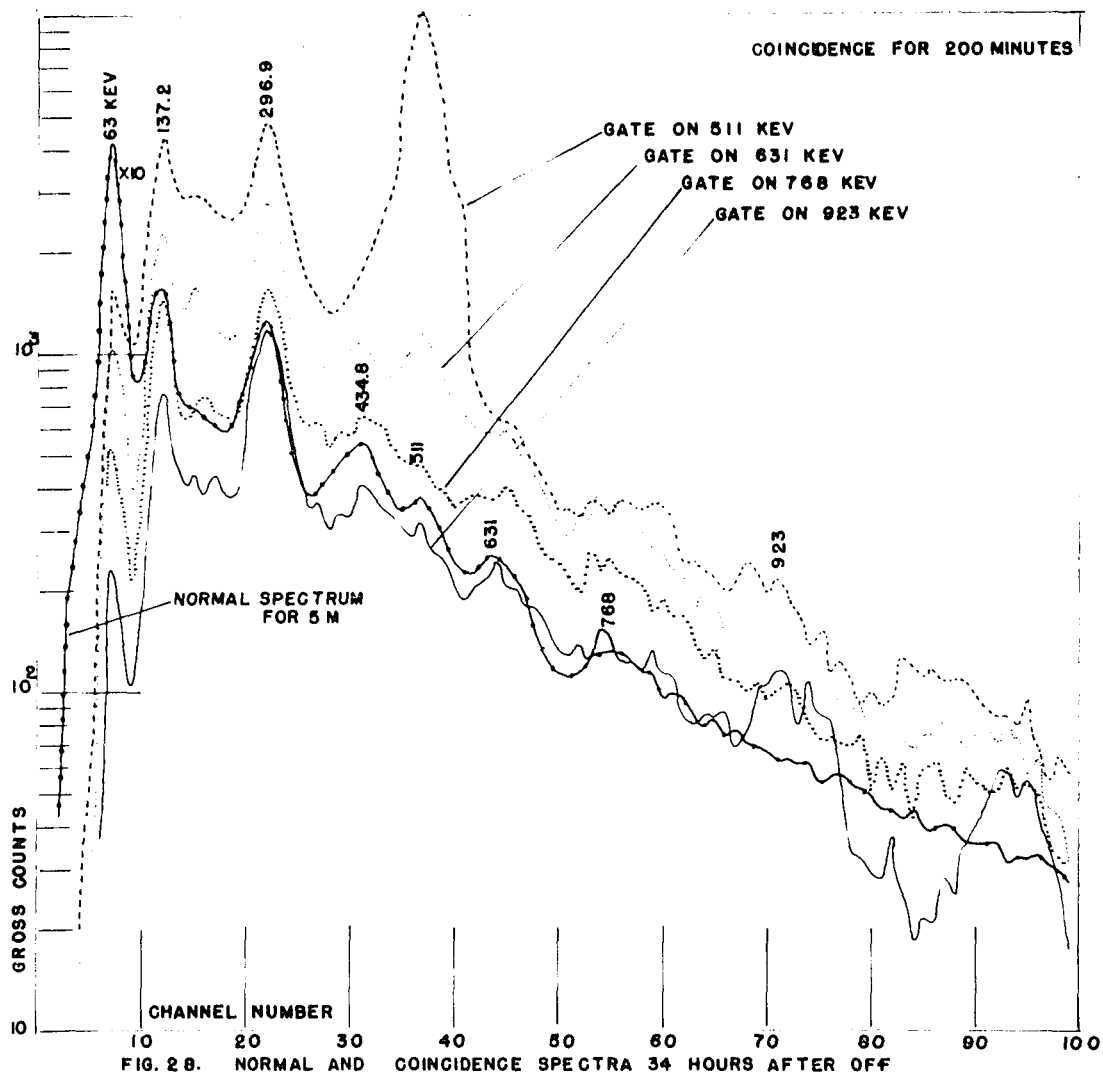

FIG. 28. NORMAL AND COINCIDENCE SPECTRA 34 HOURS AFTER OFF

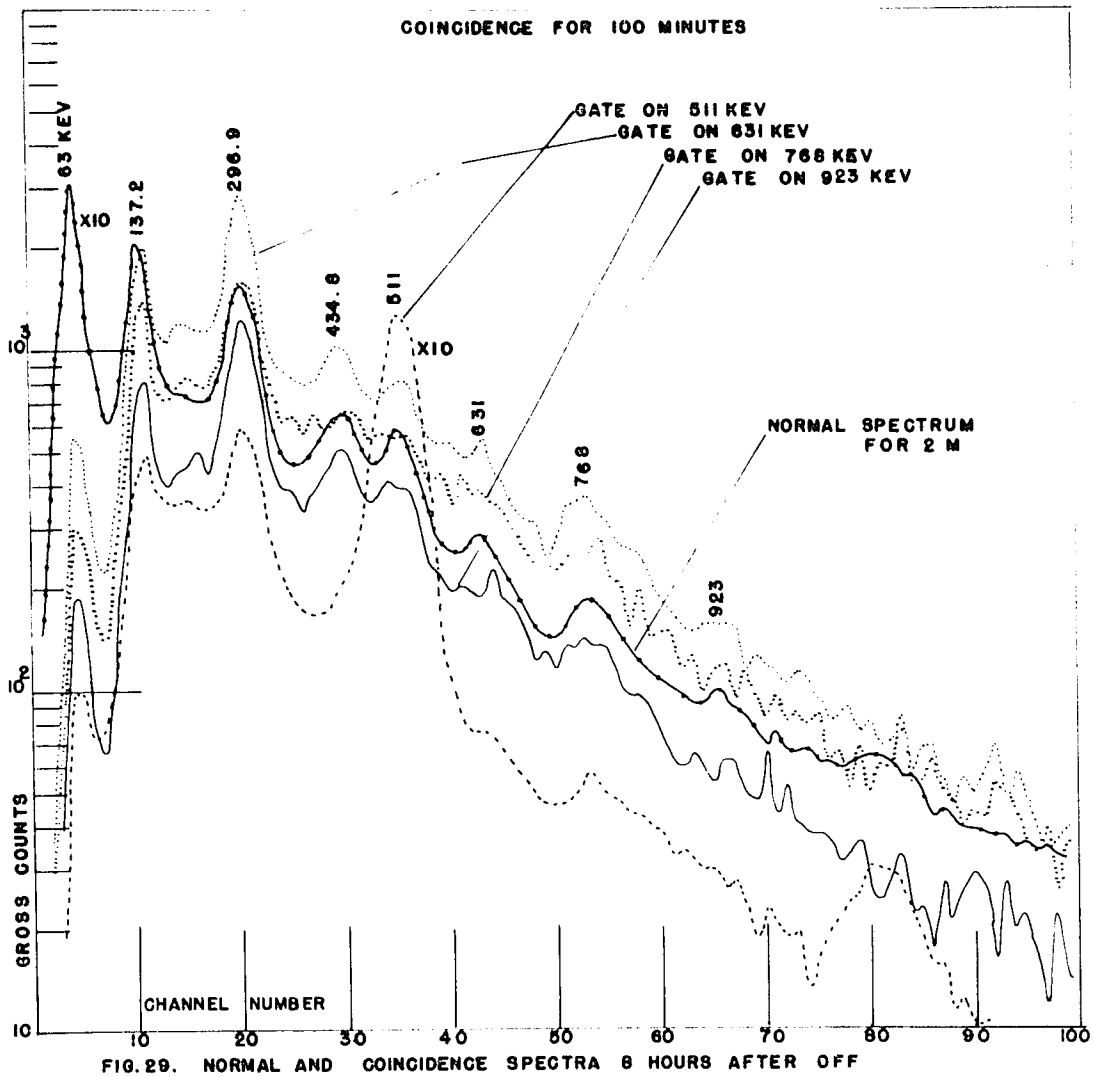

FIG. 29. NORMAL AND COINCIDENCE SPECTRA 8 HOURS AFTER OFF

Table VIII. Results Of Coincidence

	63 kev	137.2 kev	296.9 kev	434.8 kev	511 kev	631 kev	768 kev	923 kev
63 kev		yes	yes	yes		yes	yes	yes
137.2	yes		yes	yes	yes	yes	yes	yes
296.9	yes	yes		yes	yes	yes	yes	yes
434.8	yes	yes	yes		yes	yes		
511		yes	yes	yes				
631	yes	yes	yes	yes				
768	yes	yes	yes					
923	yes	yes	yes					

4. DISCUSSION

The energy level diagram of the decay of 15 h $_{77}Ir^{186}_{109}$ is given in figure 30.

Energies 137.2, 296.9, 434.8, 631, 768, and 923 kev had already been observed experimentally[3,4] as to be from 15-hour activity of Ir^{186}. Since the disintegration energy available is 3.8 mev, more energetic transitions could be expected to exist. In this work careful studies in the high energy region revealed existence of nine more transitions: 1.17, 1.33, 1.66, 2.03, 2.17, 2.36, 2.53, 2.65, and 2.79 mev with an experimental accuracy of $\pm$20 kev. In ascribing an energy peak to 15-hour Ir^{186} activity, much consideration was given to its half-life determination and relative predominance over other activities. Near the farthest end of the spectrum the separation of the energy peaks was very poor and graphical unscrambling was used as an useful tool for their identification.

In the determination of the intensity, the graphical unscrambling cannot claim very much accuracy, particularly in the high energy region where double and single escape peaks take an important part in pulse-height distribution. Yet, unscrambling reveals, at least, the order of transition which plays an important role in the decay scheme.

Coincidence data for the lowest three energies 137.2, 296.9, and 434.8 kev produce a level scheme agreeing with that of Diamond and Hollander.[4] Three other previously reported gamma rays 631, 768, and

923 kev produce a coincidence result which could not be fitted in as it was in the observed Re^{186} decay.[7] 631 kev seems to be in coincidence with 137.2, 296.9, and 434.8 kev and thus produces an energy level 1.500 mev which agrees well with $K=0^+$ $I=8^+$ state of collective excitation model. 768 and 923 kev are clearly in coincidence with 137.2 and 296.9 kev showing two other new levels at 1.202 and 1.357 mev. Energy levels suggested by Dzhelepov and Peker[13] corresponding to $K=2^+$ and $I=2^+$, 3^+, 4^+ could not be fitted in the observed data.

Coincidence data for high energies are not dependable enough for a reasonable interpretation. These high energies and their relative transition probabilities are compared and matched and a possible scheme for them has been suggested.

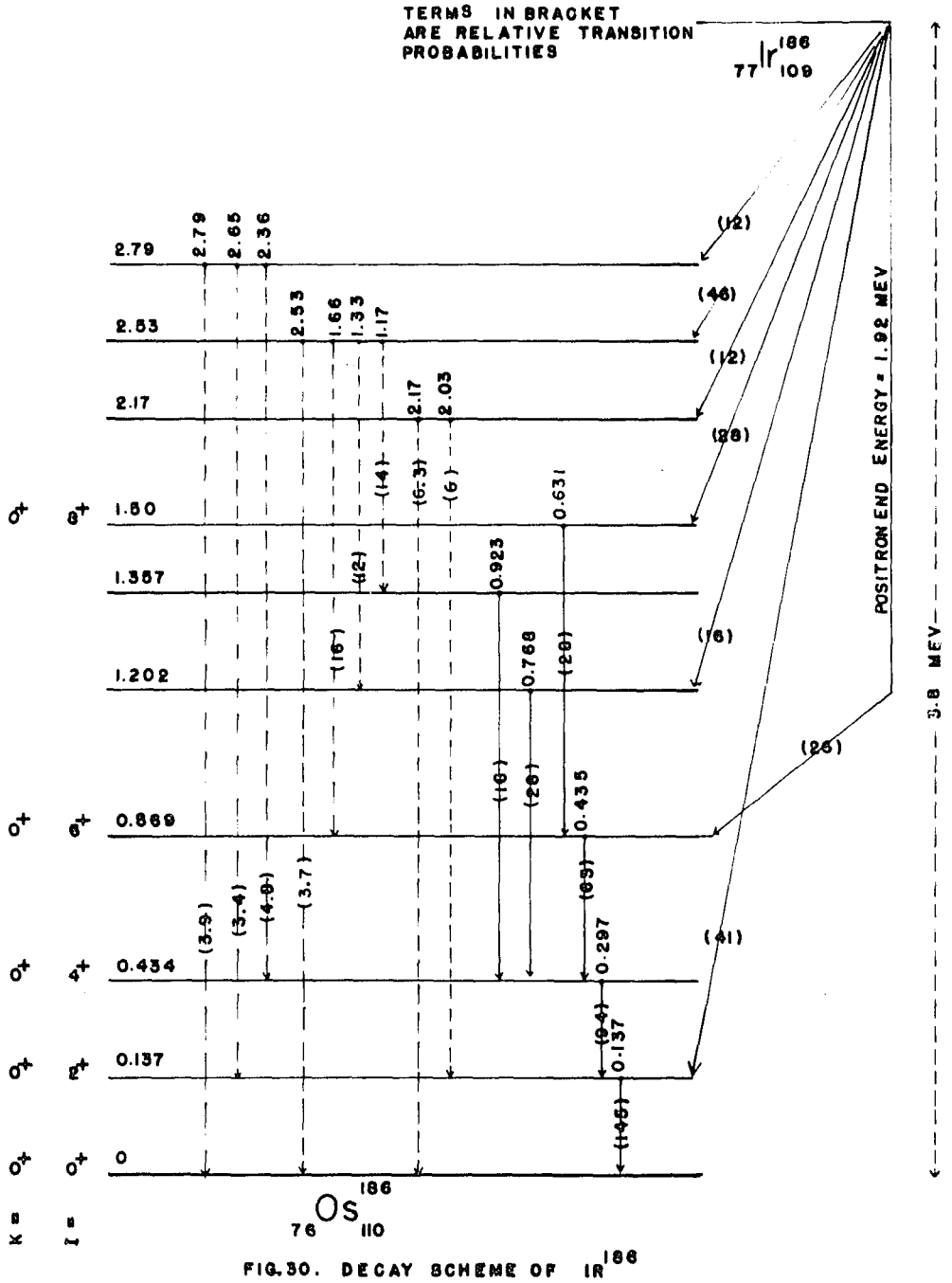

FIG. 30. DECAY SCHEME OF Ir^{186}

REFERENCES

1. C. J. Gallagher, Jr., and V. G. Soloviev, Mat. Fys. Skr., Dan. Vid. Selsk. 2, No. 2 (1962).

2. A. Bhor and B. R. Mottelson, Mat. Fys. Medd., Dan. Vid. Selsk. 27 (1953). No. 16.

3. W. G. Smith and J. M. Hollander, Phys. Rev. 98 (1955) 1258.

4. R. M. Diamond and J. M. Hollander, Nu. Phys. 8 (1958) 143.

5. F. R. Metzger and R. D. Hill, Phys. Rev. 81 (1951) 300L
   82 (1951) 646.

6. R. M. Steffen, Phys. Rev. 82 (1951) 827.

7. M. W. Johns, C. C. McMullen, I. R. Williams and S. V. Nablo, Can. J. Phys. 34 (1956) 69.

8. R. L. Heath, AEC Research and Development Report, I.D.O.-16408 (1957).

9. N. H. Lazar, IRE Trans. On Nuclear Science, NS-5, 138 (1958).

10. M. R. Bhat, Ph.D. Thesis (1961) Ohio State University.

11. M. E. Rose, Internal Conversion Coefficients (North-Holland Pub. Co. Amsterdam, 1958).

12. A. H. Wapstra, G. J. Nijgh and R. Van Lieshout, Nuclear Spectroscopy Tables (North-Holland Pub. Co., Amsterdam, 1959).

13. B. S. Dzhelepov and L. K. Peker, Vozbuzdennye Sostoyaniya Deformirovannykh Yader (Excited States of Deformed Nuclei) Joint Institute of Nuclear Research, Dubna, U.S.S.R.

14. P. R. Bell, β and γ-ray Spectroscopy, K. Siegbahn ed., p. 161 North-Holland Pub. Co., Amsterdam (1955)

AUTOBIOGRAPHY

I, Binayak Ghosh, was born in Calcutta, India, on May 23, 1932. I had my high school education in The Scottish Church Collegiate School, Calcutta from which I passed Matriculation Examination in 1948. From The University of Calcutta I had my Bachelor of Science Degree in 1953 and Master of Science Degree in 1955. In 1958 I joined The Ohio State University as a graduate student in the Department of Physics and Astronomy and since then have been in continuous residence for four years while fulfilling the requirements for the degree of Doctor of Philosophy.